https://doi.org/10.5194/acp-2022-733
Preprint. Discussion started: 23 November 2022

Atmospheric Chemistry and Physics Discussions

Re-evaluating cloud chamber constraints on depositional ice growth in cirrus clouds– Part 1: Model description and sensitivity tests

Kara D. Lamb[1], Jerry Y. Harrington[2], Benjamin W. Clouser[3], Elisabeth J. Moyer[3], Laszlo Sarkozy[3], Volker Ebert[4,5], Ottmar Möhler[6], and Harald Saathoff[6]

[1]Department of Earth and Environmental Engineering, Columbia University, New York, NY, USA
[2]Department of Meteorology and Atmospheric Science, The Pennsylvania State University, University Park, PA, USA
[3]Department of the Geophysical Sciences, University of Chicago, Chicago, IL, USA
[4]Physikalisch-Technische Bundesanstalt (PTB), 38116 Braunschweig, Germany
[5]Institute of Physical Chemistry (PCI), University of Heidelberg, 69120 Heidelberg, Germany
[6]Institute of Meteorology and Climate Research, Karlsruhe Institute of Technology, Karlsruhe, Germany

Correspondence: Kara Lamb (kl3231@columbia.edu)

Abstract. Ice growth from vapor deposition is an important process for the evolution of cirrus clouds, but the physics of depositional ice growth at the low temperatures (<235 K) characteristic of the upper troposphere/lower stratosphere is not well understood. Surface attachment kinetics, generally parameterized as a deposition coefficient α_D, are expected to limit growth rates in certain cases, but significant discrepancies between experimental measurements have not been satisfactorily explained. Experiments on single ice crystals have previously indicated the deposition coefficient is a function of temperature and supersaturation, consistent with growth mechanisms controlled by the crystal's surface characteristics. Here we use observations from cloud chamber experiments in the AIDA Aerosol and Cloud Chamber to evaluate surface kinetic models in realistic cirrus conditions involving rapidly changing temperature, pressure, and ice supersaturation, so that depositional ice growth may evolve from diffusion-limited to surface kinetics-limited over the course of a single experiment. In part 1, we describe the adaptation of a Lagrangian parcel model with the Diffusion Surface Kinetics Ice Crystal Evolution (DiSKICE) model (Zhang and Harrington, 2014) to the AIDA Chamber experiments. We compare the observed ice water content and saturation ratios to that derived under varying assumptions for ice surface growth mechanisms for experiments simulating ice clouds between 180 and 235 K and pressures between 150 and 300 hPa. We found that both heterogeneous and homogeneous nucleation experiments at higher temperatures (> 205 K) could generally be modeled consistently with either a constant deposition coefficient or with the DiSKICE model assuming growth via abundant surface dislocations. Lower temperature experiments showed more significant deviations from any depositional growth model, with different ice growth rates for heterogeneous and homogeneous nucleation experiments.

1 Introduction

Depositional ice growth from vapor is an important microphysical process for cirrus cloud formation. Cirrus clouds form in the pure ice regime (< 235 K), where water in the vapor phase condenses onto ice crystals initially formed either heterogeneously (requiring an aerosol to act as an ice nuclei, IN) or homogeneously (dependent on the water activity of super-cooled aqueous

https://doi.org/10.5194/acp-2022-733
Preprint. Discussion started: 23 November 2022


Atmospheric Chemistry and Physics Discussions

aerosol droplets (Koop et al., 2000)). Models of cirrus cloud formation have demonstrated that the value of this deposition coefficient would impact the number density of ice crystals formed through homogeneous nucleation (Lin et al., 2002; Gierens et al., 2003), the steady-state supersaturation within clouds (Zhang and Harrington, 2015), and would also have important implications for the radiative properties of cirrus clouds. Recent measurements of the surface complexity observed for small ice crystals in cirrus clouds during atmospheric field campaigns was estimated to have an additional -1.12 W/m^2 cooling effect on the earth's radiative budget (Järvinen et al., 2018). This study only investigated the impact of ice crystal surface complexity on the optical properties of ice, and did not assess its impact on depositional growth rates, which would have additional implications for the persistence and lifetime of cirrus clouds, as well as their potential to dehydrate air entering the stratosphere (Randel and Jensen, 2013).

The habits and growth rates of ice crystals have long been known to sensitively depend on temperature, pressure, and supersaturation, although the surface effects controlling vapor deposition are complex and challenging to characterize experimentally. While the faceted growth of ice at temperatures warmer than 253 K has been explained through the temperature dependence of surface ledge formation leading to the dominance of different growth mechanisms (Libbrecht, 2005), the growth mechanisms that control vapor attachment kinetics at temperatures lower than 233 K have not been directly measured and remain relatively unknown (Nelson, 2005).

Ice surface kinetic effects in cirrus clouds have often been parameterized in models as a constant deposition coefficient (α_D), with $\alpha_D \ll 1$ parameterizing very inefficient growth, and $\alpha_D \rightarrow 1$ very efficient growth (Lin et al., 2002; Gierens et al., 2003). However the increasing complexity of ice crystal habits as a function of size observed in atmospheric cirrus clouds (Schmitt et al., 2016; Magee et al., 2021) indicate a constant deposition coefficient cannot represent ice surface processes during all phases of a crystal's growth cycle. Indeed, the evolution of crystal shapes requires deposition coefficients that are not unity (e.g. Lamb and Scott (1974); Libbrecht (2003)). Recent progress on modeling surface kinetic processes on faceted single crystalline ice has been made with the development of the Diffusion Surface Kinetics Ice Crystal Evolution (DiSKICE) model, which approximates ice with two semi-axes to model crystal habits, allowing for different ice aspect ratios to be consistently modeled during depositional ice growth (Zhang and Harrington, 2014). The theory can capture the growth of crystals with various aspect ratios using a single, supersaturation and temperature dependent deposition coefficient (Harrington et al., 2019), which may make it amenable to modeling more complex crystal forms (Pokrifka et al., 2020).

Various types of experiments have been used to study surface effects during depositional ice growth. Single crystal experiments at warmer temperatures (between 233 K and 273 K) are often performed at low pressures to limit diffusive effects. Such studies have indicated the deposition coefficient is a complicated function that depends on the surface supersaturation, the temperature, the presence of chemical impurities, and the structure of the crystal surface (Nelson and Knight, 1998; Libbrecht and Rickerby, 2013; Harrison et al., 2016). However, extrapolating from single crystal experiments performed in controlled conditions to atmospheric cirrus is not straightforward, as ice crystals growing in the atmosphere compete for available vapor and experience significant changes in ambient conditions due to dynamic processes, such as the influence of gravity waves (Spichtinger and Krämer, 2013; Jensen et al., 2016; Dinh et al., 2016). These processes will affect the thermal and water vapor environment of the growing crystals, and therefore may influence the manner in which the crystals grow.

https://doi.org/10.5194/acp-2022-733
Preprint. Discussion started: 23 November 2022


Atmospheric Chemistry and Physics Discussions

Additionally, only a few studies have specifically targeted ice growth at temperatures colder than 233 K (Pratte et al., 2006; Magee et al., 2006; Bailey and Hallett, 2009, 2012) and, to date, no studies have been done on the growth of individual ice facets at these temperatures. Atmospheric measurements have also been used to constrain the deposition coefficient, although there are significant challenges in measuring ice crystal growth rates from an airborne platform, as the evolution of crystal growth over time cannot be directly measured (Kaufmann et al., 2018; Krämer et al., 2020).

One previous study (Skrotzki et al., 2013) focused on measurements of the deposition coefficient at cirrus-relevant temperatures (190-230 K) inside of a cloud chamber, where the evolution of an air parcel can be monitored over time. Cloud chambers simulate cirrus clouds formed in the atmosphere via adiabatic expansion experiments, by rapidly changing temperature and pressure to create ice supersaturated conditions. While single particle experiments have indicated the deposition coefficient can in some cases by very small (Magee et al., 2006) these cloud chamber experiments suggested deposition coefficients in cirrus conditions are near 1, and therefore can generally be neglected in model calculations of mass growth. However, calculating the shape evolution of faceted crystals, even complex ones, would still require estimating the facet-dependent deposition coefficients even if they are high. Several attempts have been made to explain the discrepancies between different experimental measurements of the deposition coefficient (Libbrecht, 2004; Harrison et al., 2016), but the questions of how these experiments can be reconciled, and whether cirrus clouds form in conditions where surface effects significantly limit growth rates, still remain.

To address these questions, we re-examine expansion experiments performed inside of the AIDA Aerosol and Cloud chamber to investigate whether depositional ice growth models including surface kinetic processes that vary with changes in ambient conditions are consistent with the observed ice growth rates. These experiments included cases of both homogeneous and heterogeneous ice formation to investigate the role of ice nucleation pathways on depositional growth. While Skrotzki et al. (2013) explored the variability in the deposition coefficient derived from experiments performed at various temperatures and with two types of heterogeneous ice nuclei, the analysis method implicitly assumed that α_D remained constant during a single expansion experiment, investigating only the constant parameterization typically used in cloud models. Recent advances in modeling surface kinetic processes on faceted ice in cirrus clouds (Zhang and Harrington, 2014, 2015) and in experimental measurements of individual ice crystals (Pokrifka et al., 2020) provide motivation to reanalyze these experiments. In this paper (Part 1) we describe the adaptation of a parcel model including different models for surface kinetic effects to the AIDA experiments (Zhang and Harrington, 2014, 2015), and compare predicted ice growth rates under varying assumptions for surface kinetic effects. In a companion paper (Part 2) we plan to quantitatively evaluate constraints placed on surface kinetic models at low temperatures by these experiments using Bayesian parameter estimation (as in e.g. Schrom et al. (2021)). Here, we discuss models for depositional ice growth from vapor and how the effects of different ice surfaces are parameterized in Section 2. We then discuss the experimental protocol and experiments performed in AIDA in Section 3. In Section 4, we discuss average observed ice growth rates and describe the adaptation of a parcel model with the different models for depositional ice growth to AIDA. In Section 5, we compare observed ice growth rates with predicted ice growth under different assumptions for surface kinetic effects. Finally we discuss the implications of these results for atmospheric cirrus cloud models in Section 6.

https://doi.org/10.5194/acp-2022-733
Preprint. Discussion started: 23 November 2022

Atmospheric Chemistry and Physics Discussions

2 Models for depositional ice growth in cirrus conditions

In single crystalline form, atmospheric ice nucleates and then subsequently grows through vapor deposition as hexagonal ice (I_h), with 2 basal (hexagonal) faces and 6 prism (rectangular) faces. The simplest model for depositional ice growth is a capacitance model, which determines mass transfer based on differences between surface temperature and far-field supersaturation (Pruppacher et al., 1998). The single crystal growth rate $\frac{dm}{dt}$ in this model is

$$\frac{dm}{dt} = -4\pi D_v f_v A_i C(c,a)(1 - S_i)\rho^{\infty}_{v,sat}, \tag{1}$$

where D_v is the molecular diffusivity of water vapor in air, A_i is a transfer coefficient incorporating the effects of heat and vapor transport, f_v is the ventilation coefficient, $C(a,c)$ is the capacitance (which depends on a and c, half the longest distance along the basal and prism facets, respectively), S_i is vapor saturation over ice, and $\rho^{\infty}_{v,sat}$ represents the water vapor density at saturation over ice at the far field temperature (i.e. far from the growing ice crystal) (Mason, 1971). A_i is a function of both the thermal conductivity k_T and the vapor diffusivity D_v. In the classical capacitance model, perfect attachment kinetics are implicitly assumed. A consequence of this assumption is that the vapor density is constant over the crystal surface. This surface condition is inconsistent with the growth of any kind of facet, since faceting requires α_D that are less than unity and a vapor density that varies across the crystal facet (Nelson and Baker, 1996).

Ice growth requires consideration of mass and thermal energy transfer through the background gas along with molecular attachment onto the crystal surface. Small ice crystals characteristic of those that form immediately following homogeneous nucleation (<20 μm) in cirrus clouds will also be influenced to some extent by attachment kinetics, especially as facets emerge during growth (Harrington and Pokrifka, 2021). The capacitance model can be modified to include these attachment kinetics by assuming growth occurs across two regions: a continuum region, where gases can be modeled as a continuous fluid and diffusion theory applies, and a kinetic region at the surface of the crystal where gases act as their individual component molecules and surface uptake reduces growth (Pruppacher et al., 1998). The boundary between the two regions is the vapor jump length Δ_ρ, which is generally assumed to be the mean free path λ_w of a water molecule in air. The surface effects are included as a modified diffusivity D^*_w and a modified thermal conductivity k^*_T, which are functions of the deposition coefficient α_D and the thermal accommodation coefficient α_T. This latter quantity is thought to be near unity, but it has not been measured at low temperatures.

When surface ledge densities are high enough that they do not impede growth, the deposition coefficient becomes equivalent to a molecular adsorption/desorption efficiency, e.g. a molecular "sticking" coefficient, where

$$\alpha_D = \alpha_s \tag{2}$$

and α_s is the probability that an incident molecule will adsorb to the crystal surface, i.e. α_s is a constant between 0 and 1. This adsorption efficiency is generally considered to be near unity ($\alpha_s \sim 1$) (Libbrecht, 2005). Experiments using a molecular beam to study the adsorption and desorption of D_2O on H_2O ice surface found a value of 0.41±0.81 for the adsorption efficiency at 200 K and an indication that α_s decreases with increasing temperature (Kong et al., 2014a).

https://doi.org/10.5194/acp-2022-733
Preprint. Discussion started: 23 November 2022

Atmospheric Chemistry and Physics Discussions

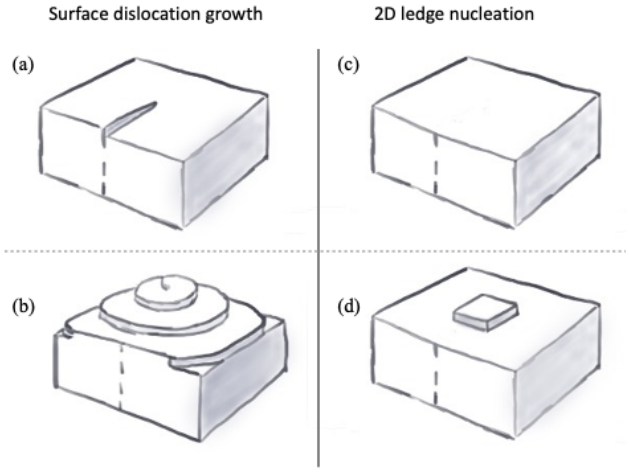

Figure 1. Examples of crystal surface structure. One-dimensional defects in the crystal lattice (a) provide favorable attachment sites that lead to screw dislocations (b). When no defects are initially present (c), 2D ledges must first form on the crystal surface to provide favorable attachment sites (d).

The constant parameterization for the deposition coefficient (Eq. 2) does not physically account for the diffusion of molecules across the face of the crystal to favorable attachment sites, however. Statistical mechanical considerations indicate that crystal growth through vapor deposition is a function of the structure of the crystal surface, as attachment of vapor molecules to surfaces without pre-existing ledges is not energetically favorable. Ice crystals often form with one-dimensional defects in the crystal lattice leading to the occurrence of screw dislocations (Figure 1a,b). The occurrence of these defects provide attachment sites for vapor depositing on ice, leading to characteristic spiral growth patterns (Burton et al., 1951). Facets without ledges require the nucleation of 2-dimensional "islands", or ledges to provide favorable attachment sites (Figure 1c,d). The deposition coefficient associated with both growth mechanisms has been shown to be dependent on the ratio of the local supersaturation s_{local} to a critical supersaturation s_{crit}, with very inefficient vapor deposition associated with 2D ledge nucleation when $s_{local} < s_{crit}$, while screw dislocation growth has a much more gradual dependence (Burton et al., 1951). These growth mechanisms have been observed experimentally, e.g. through advanced optical microscopy of basal and prism facets of ice grown near the melting point (Sazaki et al., 2010, 2014). Other types of crystal defects, such as stacking faults (planar crystal defects), can also act as favorable attachment sites (Nelson and Baker, 1996).

The deposition coefficient for the growth processes described above can be parameterized using a relatively simple model proposed by Nelson and Baker (1996). This model parameterizes the surface diffusion of molecules to ledges or steps that form on the crystal surfaces (Nelson and Baker, 1996), and is an explicit function of the surface supersaturation and properties of the crystal surface, and an implicit function of temperature through the critical supersaturation, $s_{crit}(T)$. Vapor attachment kinetics include both the diffusion time scale across the crystal surface to favorable attachment sites and the relative probability

https://doi.org/10.5194/acp-2022-733
Preprint. Discussion started: 23 November 2022

Atmospheric Chemistry and Physics Discussions

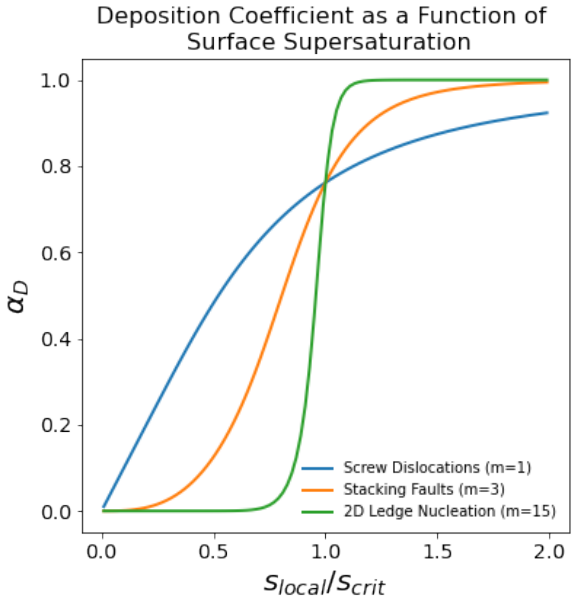

Figure 2. The deposition coefficient as a function of surface supersaturation. Crystals growing via vapor deposition may support different types of growth mechanisms resulting from properties of the crystal surface (e.g. screw dislocations, stacking faults, or 2D ledge nucleation). The deposition coefficient is therefore expected to be a function of the surface supersaturation (s_{local}) relative to a critical supersaturation (s_{crit}). This critical supersaturation is generally considered to be a function of the crystal facet (basal or prism) and the temperature.

that a molecule will be incorporated into the crystal lattice. Deposition is often parameterized in this case as,

$$\alpha_D = \alpha_s \left(\frac{s_{local}}{s_{crit}} \right)^m tanh \left[\left(\frac{s_{crit}}{s_{local}} \right)^m \right] \tag{3}$$

where s_{local} is the supersaturation just above the crystal surface (Nelson and Baker, 1996). The adsorption efficiency α_s is generally taken to be unity (see above). Growth mechanisms on ice surfaces are parameterized using different values for m (See Figure 2). Growth by permanent surface dislocation (Burton et al., 1951) is parameterized by a value of $m = 1$, stacking fault-induced nucleation as $m \sim 3-5$ (Ming et al., 1988), and 2D ledge nucleation as $m \sim 10-15$ (Nelson and Baker, 1996). In cloud models and global climate models, even when the sensitivity with respect to the deposition coefficient has been explored, it has generally been varied as a constant value (Eq. 2) and not consistently with the ice surface growth mechanisms (Eq. 3) (Nelson, 2005).

This deposition coefficient is valid for the faceted growth of ice crystals into the variety of habits observed in the atmosphere (Burton et al., 1951; Lewis, 1974; Lamb and Chen, 1995). For I_h, the basal and prism facets have been shown to have different deposition coefficients, with distinct dependencies on temperature and supersaturation, consistent with large variety of ice crystal morphologies observed in the atmosphere. Additional branching and faceting instabilities are also important, leading to the dendritic growth and hollowing observed in snow crystals (Wood et al., 2001; Libbrecht, 2005). Recent single crystal

https://doi.org/10.5194/acp-2022-733
Preprint. Discussion started: 23 November 2022

Atmospheric Chemistry and Physics Discussions

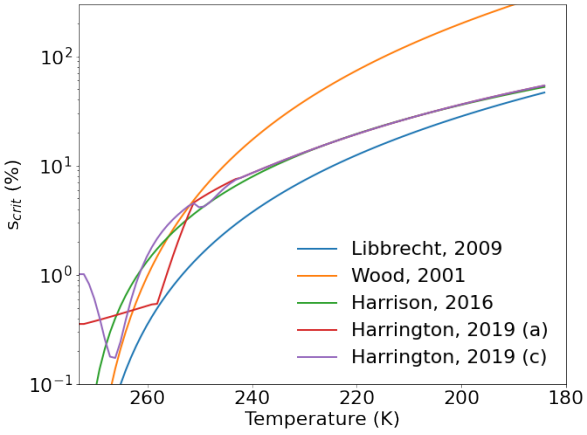

Figure 3. Temperature dependence of s_{crit}. Parameterizations for the temperature dependence of s_{crit} that we compare in this study.

experiments have generally focused on the determination of s_{crit} for the basal and prism facets (Nelson and Knight, 1998; Libbrecht and Rickerby, 2013; Harrison et al., 2016), although all of these experiments have focused on measurements at $T >$233 K. Figure 3 shows parameterizations for s_{crit} as a function of temperature. The values below 233 K are extrapolations (Wood et al., 2001; Libbrecht and Arnold, 2009; Harrison et al., 2016) and rough estimates from prior data (Harrington et al., 2019).

Additional complications for ice deposition arise due to the presence of chemical impurities or coatings on ice surfaces (Libbrecht, 2005). Molecular beam experiments further indicated near unity accommodation of water vapor on nitric acid and acetic acid coated ice, but more efficient desorption in the case of short-chain alcohols (Kong et al., 2014b). Previous studies have also demonstrated differences in ice crystal morphologies due to the presence of chemical impurities (Hallett and Mason, 1958; Mason, 1971).

2.1 Impacts of nucleation pathways on depositional growth rates

Recent experimental work suggests that depositional ice growth rates (Bailey and Hallett, 2002; Harrison et al., 2016; Pokrifka et al., 2020; Harrington and Pokrifka, 2021) and surface complexity (Schnaiter et al., 2016; Voigtländer et al., 2018) may be impacted by whether heterogeneous or homogeneous nucleation initiates the ice growth process. Prior to nucleation, experiments on heterogeneous ice nuclei have demonstrated surface defects on mineral dust serve as active sites for growth (Kiselev et al., 2016). Differences in the morphology of mineral dust has also been shown to impact the number of active sites available for nucleation (Hiranuma et al., 2014a, b). Homogeneous nucleation instead is dependent on a phase transition leading to crystallization in supercooled aqueous droplets, which occurs spontaneously without requiring preferential nucleation sites. Following nucleation, these different processes may lead to ice crystals with distinct surface characteristics. Ice formed as a

https://doi.org/10.5194/acp-2022-733
Preprint. Discussion started: 23 November 2022


Atmospheric Chemistry and Physics Discussions

result of heterogeneous nucleation has been suggested to be dominated by dislocation growth (Harrison et al., 2016), whereas measurements also suggest that homogeneously nucleated ice is initially dominated by dislocations but may rapidly transition to ledge nucleation growth (Pokrifka et al., 2020).

Because higher supersaturations are required for homogeneous nucleation, ice crystals formed via heterogeneous or homogeneous nucleation mechanisms experience different histories of supersaturation. This higher supersaturation required to nucleate ice homogeneously could lead to a "kinetic roughening" of the ice surface (Libbrecht, 2005). Additionally, recent single crystal experiments of ice formed through homogeneous nucleation on Snowmax indicated that a growth transition may occur during growth in conditions of constant supersaturation, with initial growth occurring efficiently and later growth inefficiently (Pokrifka et al., 2020). Ice crystal complexity, defined as the sub-micron surface structure of ice, varies as the crystals grow, with differences between heterogeneous and homogeneous nucleation observed during adiabatic expansion experiments in AIDA (Schnaiter et al., 2016; Järvinen et al., 2018). Homogeneous nucleation experiments were found to create highly complex ice, whereas heterogeneous nucleation experiments lead to ice varying from pristine (molecularly smooth) to highly complex as a function of the supersaturation. Because the deposition coefficient depends on the relative smoothness of the ice crystal surface, these results suggest homogeneous and heterogeneous nucleation may create ice with unique deposition coefficients.

3 Cloud chamber experiments of depositional ice growth for T<235 K

To investigate depositional ice growth at low temperatures, cirrus cloud simulation experiments were performed in the AIDA Aerosol and Cloud Chamber during the IsoCloud 4 campaign in March 2013. The IsoCloud experiments consisted of a series of pseudo-adiabatic expansion experiments between 180-235 K, and the experimental protocol used during the campaigns has been previously described in (Lamb et al., 2017; Clouser et al., 2020). AIDA is a large chamber (84.5 m^3 volume) where mixed phase and ice clouds can be experimentally simulated through adiabatic expansion of air (a synthetic mixture of N_2, O_2, and Ar) and water vapor. This adiabatic expansion cools the gas inside the chamber by several degrees Kelvin, leading to conditions of ice supersaturation sufficient to nucleate ice, either by introducing solid aerosol particles (to nucleate ice heterogeneously) or aqueous aerosol droplets (to nucleate ice homogeneously).

In a typical expansion experiment, the cloud chamber is prepared by initially cooling the entire sample volume to a starting temperature < 235 K. This cooling takes several hours and therefore each experimental day focused on a series of 4-7 experiments performed with similar starting temperatures. The IsoCloud campaign included experiments over 9 days, for a total of 48 expansion experiments.

To prepare the chamber walls with a thin layer of ice, water vapor was initially sprayed into the chamber and then the chamber was pumped down, with this process repeated several times to provide a reasonably uniform coverage of the walls with a thin ice coating. The ice on the walls helps maintain equilibrium conditions with the water in the vapor phase (with the gas initially at a slightly higher temperature than the chamber walls, producing ice sub-saturated conditions with RH_i ~80-90%).

https://doi.org/10.5194/acp-2022-733
Preprint. Discussion started: 23 November 2022

Atmospheric Chemistry and Physics Discussions

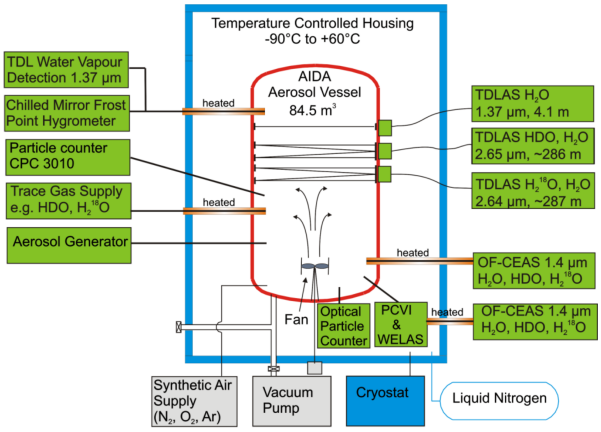

Figure 4. AIDA measurement chamber and instrumentation during the IsoCloud Campaigns. The AIDA chamber is a large volume (84.5 m^3) environmental chamber. Pressure can be dynamically controlled via vacuum pumps evacuating gases and particles, leading to adiabatic cooling of the gas. A fan circulates air inside the chamber to mitigate gravitational settling and mix the air inside the chamber. The instrumental layout during the IsoCloud experiments is shown, with the TDL instruments (ChiWIS and SP-APicT) measuring water vapor approximately 2/3rds of the height of the chamber, and the welas optical particle counters measuring near the bottom of the chamber. Total water was monitored (by APeT) via extraction along a heated inlet at approximately the same height as the water vapor instruments.

Ice cloud experiments were performed with several different types of aerosols to create a range of conditions to investigate ice growth inhibition at low temperatures. Before the start of an expansion experiment, aerosols were introduced into the chamber. Arizona Test Dust (ATD), a mineral dust proxy, was used in 31 experiments, as it has previously been shown to be a very efficient heterogenous IN, with an ice active fraction between 0.6-0.8 for S_i<1.15 at T=209 and 223 K (Möhler et al., 2006). ATD particles were size selected via impaction for sizes < 2 μm and were dispersed via a rotating brush generator (RGB 1000, PALAS) (Möhler et al., 2006). Aqueous sulfuric acid particles (H_2SO_4/H_2O, referred to hereafter as SA) were generated as in (Wagner et al., 2008) and were used in 9 experiments. Secondary organic aerosol (SOA) was used for 1 experiment with an additional 3 experiments using SOA coated with nitric acid. Atmospheric observations and laboratory measurements have previously shown that nitric acid may impede ice growth in cirrus conditions (Gao et al., 2004, 2015). Reference pumpdowns (e.g. without any aerosols added) were performed in 6 cases; the typical aerosol background concentrations in AIDA is less than 0.1 cm^{-3}.

After ice formation, the ice on the walls provide an additional source of water vapor to the chamber. In a typical experiment, pumping occurs over 5-10 minutes, and after the end of pumping, the ice evaporates after ∼10 minutes, as a heat flux through the chamber walls warms the gas inside. A mixing fan inside the chamber is used to mediate the impacts of gravitational settling during the course of the expansion experiment, as well as to decrease inhomogeneity in the gas. The mixing time scale is on the order of 30 s. The gases and aerosols introduced into the chamber are diluted by a factor of ∼2 while the pumps are turned on. Gas temperature is measured by 5 thermocouples located along a wire at different heights approximately 1 m from

https://doi.org/10.5194/acp-2022-733
Preprint. Discussion started: 23 November 2022

Atmospheric Chemistry and Physics Discussions

Table 1. Optical instruments used in analysis. The range for Chi-WIS, SP-APicT, APeT indicate the temperature range over which the instrument can generally be used to retrieve water vapor mixing ratios. For APeT, ice crystals greater than 7 μm are sampled with less than 100% efficiency. The range for the welas instrument indicates the effective spherical radius of the particles that can sampled, although this is dependent on morphology and orientation of the crystals in the instrument.

Instrument	Observable	Range	Time Resolution	Accuracy	Description
Chi-WIS	H_2O, *in situ* vapor (ppmv)	190 - 235 K	1 s	±5%	TDLAS at 2.65 μm, 256-286 m optical path (Sarkozy et al., 2020)
SP-APicT	H_2O, *in situ* vapor (ppmv)	205 - 235 K	1 s	±5%	TDLAS at 1.37 μm, 4.1 m optical path (Skrotzki, 2012)
APeT	H_2O, extractive total water (ppmv)	190 - 235 K, < 7μm	1 s	±5%	TDLAS at 1.37 μm, 30.3 m optical path (Lauer, 2007; Skrotzki, 2012)
welas 1	Ice crystal number density (#/cm^3)	0.3-46 μm	5 s	±20%	Optical particle counter, PALAS 2000 (Benz et al., 2005)

the chamber walls; here we use an average of the 4 lower thermocouples, as the 5th is located near the top of the chamber and shows significantly greater temperature variability; the TDL instruments were located between the 3rd and 4th thermocouples (see Figure 4). The typical standard deviation is <0.5 K in steady-state conditions and < 1 K during the expansion experiments (at 210 K).

Instrumentation used during the campaign provided evolving aerosol and ice number concentrations, total water and water vapor mass mixing ratios, pressure, and temperature during the experiments. A schematic of the experimental set-up during the campaign is shown in Figure 4, and a summary of the instruments used in the experiments, the quantities that they measure, and their associated measurement ranges and uncertainties is given in Table 1. Water vapor was measured via tunable diode laser absorption spectroscopy (TDLAS) sampling directly within the chamber volume. SP-APicT (single pass AIDA PCI in cloud TDL) (Skrotzki et al., 2013) was used for water vapor measurements in dense clouds at warm temperatures (21 of 48 experiments), as its single pass configuration reduces attenuation due to back-scattering from ice crystals. ChiWIS (the Chicago Water Isotope Spectrometer) (Sarkozy et al., 2020) was used to measure water vapor at low temperatures, as its longer path length gives better precision below 205 K. APeT (AIDA PCI extractive TDL) (Lauer, 2007) measured total water (vapor plus ice) via extraction through a heated inlet. Water vapor instruments used in this campaign were tested during the AQUAVIT-II water vapor instrument inter-comparison campaign, and were shown to agree within ±2.5% percent (Sarkozy et al., 2020). SP-APicT and APicT were also previously evaluated during the AQUAVIT-I campaign (Fahey et al., 2014).

Uncertainties in mass mixing ratio for TDLAS measurements are generally a combination of effects due to the intrinsic precision of the instrument and other observables, and systematic, multiplicative offsets due to the molecular spectral line parameters. The ChiWIS instrument's typical precision of 22 ppbv in H_2O corresponds to relative precisions of 5% at 0.45 ppmv and 0.02% at 100 ppmv for 1 Hz measurements. In the IsoCloud campaigns, systematic errors due to uncertainties in spectral line parameters are about 3% across all experiments, and sytematic biases and uncertanties related to the instrument and its setup contribute another 1.3%. Both APeT and SP-APicT use the same spectral lines to determine water mixing ratios. For consistency, to account for differences due to spectral line strength errors, APeT and SP-APicT were scaled up by 1.5% to match ChiWIS (Clouser et al., 2020; Sarkozy et al., 2020). To determine ice water (subtracting total water from APeT by water vapor from either SP-APicT or ChiWIS), any additional offsets before the start of pumping were subtracted so that initial ice water was assumed to be 0. Additional information about the optical measurements made in AIDA are given in (Wagner et al.,

https://doi.org/10.5194/acp-2022-733
Preprint. Discussion started: 23 November 2022

Atmospheric Chemistry and Physics Discussions

Table 2. IsoCloud 4 Experiments. Summary of conditions during expansion experiments.

Date	Number	Aerosol	T_0 (K)	ΔT (K)	p_0 (hPa)	Δp (hPa)	w_{eff} (cm/s)	$r_{v,0}$ (ppmv)	$\Delta r_{v,0}$ (%)	S_i (max.)	CCN (max.)	R (μm)	Kn	Notes
3/11/13	1	ATD	234	7.8	299	65	-370	380	39	1.21	20.7			
	2	ATD	233	6.5	300	100	-130	366	17.7	1.24	8.7	5.2-10.4	0.04-0.17	
	3	ATD	233	6.4	300	101	-120	377	28.6	1.03	39.4	4.1-6.4	0.06-0.12	
	4	ATD	233	9.1	300	131	-130	375	38.2	1.21	44.0	4.4-6.3	0.05-0.64	growth and evaporation cycle
	5	ATD	233	9.1	300	132	-180	387	43.8	1.05	51.9	5.1-6.3	0.06-0.23	
3/13/13	6	ATD	223	6.6	300	71	-170	113	29	1.27	11.1	1.6-6.8	0.05-0.17	
	7	ATD	223	6.4	234	64	-140	147	35.3	1.03	93.2	2.8-3.8	0.10-0.13	
	8	ATD	223	8.7	300	131	-200	114	46.4	1.04	75.0	3.7-4.3	0.07-0.11	
	9	ATD	223	6.0	300	71	-160	114	30.7	1.12	70.4	3.0-4.5	0.08-0.43	
	10	ATD	223	5.5	231	62	-130	147	29.7	1.1	75.4	2.9-4.3	0.11-0.61	
	11	ATD	223	8.9	300	150	-180	115	47.3	1.03				
3/14/13	12	Ref.	213	5.4	298	69					7.4	5.7-10.2	0.03-0.05	
	13	ATD	213	5.3	234	64	-130	40.6	33.1	1.06	351.2	1.0-1.6	0.27-0.83	
	14	ATD	213	8.4	300	137	-160	30.9	46.8	1.04	489.9	1.0-1.6	0.11-0.61	
	15	ATD	213	5.6	300	71	-160	31.1	63.4	1.04	403.2	1.0-1.5	0.17-0.56	
	16	ATD	213	5.4	234	64	-140	39.9	32.1	1.03	455.3	1.0-1.5	0.30-1.39	
	17	ATD	213	8.4	300	130	-150	31.1	48.3	1.04	592.1	1.0-1.5	0.24-1.81	
3/15/13	18	Ref.	194											
	19	ATD	194	5.2	300	71	-120	1.78	2.2	1.87	4.3	1.5-2.0	0.13-0.19	
	20	ATD	194	4.8	239	70	-90	2.13	36.2	1.46	218.2	0.5-0.9	0.12-1.22	
	21	ATD	194	7.6	300	131	-120	1.7	53.9	1.60	302.3	0.6-0.8	0.22-1.83	
	22	ATD	194	7.4	300	131	-120	1.67	51.5	1.62	196.6	0.6-0.9	0.05-8.44	
	23	ATD	194	7.0	250	81	-180							no welas data
3/18/13	24	ATD	204	5.4	304	74	-130				218.9	0.8-13	0.07-0.35	
	25	ATD	204	4.9	233	63	-100	9.98	27.8	1.2	193.4	0.4-1.2	0.16-1.28	
	26	ATD	204	8.0	300	131	-130	7.72	49	1.27	351.6	0.5-1.1	0.06-2.17	
	27	ATD	204	8.1	300	131	-160	7.58	48.4	1.07	372.9	0.8-1.1	0.25-0.34	
3/19/13	28	Ref.	194	5.1	304	75	-120	1.6	23.6	1.67	20.6	0.8-1.6	0.18-0.49	
	29	SA	194	6.5	235	66	-140	2.04	13.2	1.84	14.9	1.4-3.5	0.04-7.61	
	30	SA	194	7.6	300	131	-140	1.65	53.4	1.88	64.5	0.6-2.0	0.12-0.40	
	31	SA	194	7.5	300	131	-150	1.78	53.3	1.95	40.3	0.8-1.5	0.14-0.56	
	32	ATD-SA	194	7.6	300	131	-140	1.74	58.7	1.34	121.2	0.9-1.1	0.07-7.49	
	33	ATD-SA	194	7.6	300	139	-120	1.55	60.4	1.34	259.2	0.8-1.5	0.15-0.40	
3/20/13	34	Ref.	189	7.3	306	136	-140	0.78	21.1	1.84	14.1	1.1-1.8	0.13-0.23	
	35	SOA	189	7.3	305	137	-140	0.73	60.9	1.88	46.8	1.0-1.8	0.07-5.28	
	36	SOA-HNO_3	189	7.3	302	134	-150	0.58	0.26	1.95				
	37	SOA-HNO_3	189	7.2	301	132	-140	0.79	0.47	1.34	258.9	0.8-1.0	0.19-22.47	
	38	SOA-HNO_3	189	7.0	301	135	-120	0.72	0.32	1.34	60.6	0.9-1.2	0.08-16.96	
3/21/13	39	Ref.	224	6.1	300	71	-120	112	1.3	1.24				
	40	ATD	224	7.6	234	65	-120	129	14.8	1.18	9.3	3.1-5.0	0.04-3.31	
	41	ATD	224	8.9	300	134	-240	103	31.4	1.24	17.2	4.0-6.1	0.07-0.09	dry walls
	42	ATD	224	8.4	300	130	-160	121	44	1.23	15.8	3.6-6.5	0.06-0.08	dry walls
	43	ATD	224	8.5	300	130	-130	128	40.3	1.12	17.2	3.2-6.3	0.06-0.08	dry walls
3/22/13	44	Ref.	204	8.0	300	71	-300	7.96	30.8	1.71	24.6	1.0-2.4	0.12-1.09	
	45	SA	205	8.3	300	134	-140	7.79	34	1.45	18.3	1.6-2.9	0.12-0.17	
	46	ATD-SA	204	5.5	301	74	-130	8.32	34	1.2	179.8	0.8-1.3	0.04-9.89	
	47	ATD-SA	204	5.2	233	64	-120	10.1	27.2	1.17	177.2	0.4-1.2	0.03-18.16	
	48	ATD-SA	204	7.6	301	132	-150	8.06	48.5	1.12	292.8	0.9-1.2	0.15-1.07	

2009). Data for each expansion experiment was synchronized to the start of pumping. ApeT was assumed to have a 17 s offset

https://doi.org/10.5194/acp-2022-733
Preprint. Discussion started: 23 November 2022


Atmospheric Chemistry and Physics Discussions

time (as was previously measured in Skrotzki et al. (2013) by looking at time differences between when *in situ* and extractive hygrometers measured a sudden change in water vapor inside AIDA).

4 Modeling depositional ice growth in AIDA

Ice growth during expansion experiments in AIDA occurs in three distinct phases: an initial nucleation phase, a growth phase, and an evaporation phase. The nucleation phase sets the condition of supersaturation during the growth phase, dependent on the availability and type of ice nuclei. Ice growth via deposition occurs while cooling is ongoing, and once the pumps have been turned off, the ice sublimates as the heat flux through the chamber walls warms the gas inside. Table 2 gives all of the experiments performed during the campaign.

Depositional ice growth can occur in three distinct regimes, depending on the growth rate limiting processes: vapor diffusion limited, surface diffusion (e.g. kinetically) limited, or heat conduction limited (Kuroda and Lacmann, 1982; Nelson and Baker, 1996). Generally heat conduction limited growth is assumed to impact warm mixed phase clouds, vapor diffusion limited growth impacts cold mixed phase clouds, and surface diffusion processes may be the limiting growth process in pure ice clouds, as we consider here (Nelson and Baker, 1996; Gierens et al., 2003).

In Table 2, we show that the IsoCloud experiments have Knudsen numbers ranging from ∼0.01 to 10, suggesting that growth should be surface kinetics limited. However, because the deposition coefficient (Eq. 3) varies as a function of s_{local}, ice growth may not be significantly limited by surface effects even in this regime, if $s_{local} \gg s_{crit}$. The relative kinetic to diffusion-limited growth rates as a function of the Knudsen number depend strongly on the surface mechanism (e.g. as shown in Figure 14 of Harrison et al. (2016)). In the case of dislocation growth, the Knudsen number still generally predicts the ice growth regimes, but for 2D ledge nucleation, ice growth can be significantly suppressed even in the case of a low Knudsen number.

To quantitatively explore surface kinetics effects during ice growth in AIDA, we use the Lagrangian parcel model with a bin microphysical scheme previously described in Zhang and Harrington (2015). This parcel model uses the DiSKICE model to determine the rate of vapor diffusion to the growing ice crystals, under different assumptions for the deposition coefficient as described in Section 2 .

4.1 Adaptation of parcel model to AIDA chamber

Lagrangian parcel models typically assume that both the mass of water is conserved between vapor, ice, and liquid phases and heat are conserved during adiabatic cooling. The AIDA chamber is not in fact a closed system, however, as there is both a heat flux through the aluminum chamber walls (2 cm thick, maintained at a constant temperature) and a reservoir of water (from ice condensed on the chamber walls). AIDA expansion experiments can be considered pseudo-adiabatic, however. To adapt the parcel model to the AIDA cloud chamber experiments, a vapor tendency term was added to the model to include the source of water vapor from the chamber walls. This vapor tendency term is estimated by assuming the change in total measured water (gas plus condensate phases) is due to the flux of water from the chamber walls (ice crystals > 7 μm are not sampled with 100% efficiency, so this may be an underestimate however) (Cotton et al., 2007). The inclusion of this term significantly improves

https://doi.org/10.5194/acp-2022-733
Preprint. Discussion started: 23 November 2022


Atmospheric Chemistry and Physics Discussions

matching between the model and observations, particularly in the latter part of each experiment when vapor flux from the walls can be significant.

For each experiment, the parcel model is initiated with the observed temperature, pressure, and ice number concentration (Figure 5). Since the OPC's have a 5 s resolution (See Table 1), we use the leading eigenmodes from a singular spectrum analysis (Vautard and Ghil, 1989) on the raw time series to reconstruct the time evolution of the ice number density, as was previously done in (Lamb et al., 2017). The initial RH_i measured by the TDL instruments are used to initiate the model. We constrain the model to the observed ice number concentration by scaling the number concentration in each bin relative to the concentration observed at that time step. This assumption preserves the mass, but leads to an increase (decrease) in the average ice particle size, relative to the decrease (increase) in ice number concentration; due to the effects of the mixing fan, sedimentation rates cannot be directly estimated from calculated particle fall speeds. The parcel model only simulates ice and water vapor, as all experiments were performed at temperatures below the homogeneous freezing limit of water (and thus we assume that liquid water would not be present in significant quantities).

To simulate the AIDA chamber, the effective vertical motion was determined from the temperature derivative as

$$w_{\text{eff}} = -\frac{dT}{dt}\frac{c_p}{g} \tag{4}$$

where w_{eff} is the effective updraft speed in m/s, $\frac{dT}{dt}$ is the time derivative of the temperature in K/s, c_p is the specific heat capacity of dry air (1004 J/(kg K)), and g is the gravitational constant (9.81 m/s^2). Typical updraft speeds in AIDA during the IsoCloud experiments were between 90-300 cm/s (See Table 2). The time derivative of the observed temperature is used to determine the effective updraft speed at each 1 second model time step.

The model is only run while the pumps are on, e.g. during the cooling phase while the pressure is decreasing, so as to model only deposition rather than sublimation. The Lagrangian parcel model runs for between 233-730 seconds. (However in most cases, the sublimation phase can be fit consistently as well, suggesting that similar physics are at play as molecules desorb from the ice.) We exclude Exp. 18 (where there was no data for several of the instruments), two experiments with very low IWC (Exp. 19, where IWC was < 0.4 ppmv and Exp. 29 where IWC was < 1.2 ppmv), three experiments at 189 K (Exp. 36-38) where APET had a significant offset from ChiWIS prior to the experiments, suggesting ice may have formed near the extractive inlet, and one experiment (Exp. 39) with very low IN concentrations (< 1 per cm^3).

5 Model results under different assumptions for surface kinetic effects

To investigate the sensitivity of depositional growth rates in AIDA to the parameterization for α_D, we performed several different simulations with the parcel model assuming different models of α_D discussed in Section 2. Since ice crystals are small ($< 20\mu$m, Table 2), here we assume that crystals have not yet developed distinctive habits, i.e. we assume that the deposition coefficients of the a and c axes of the crystals are the same; thus we do not investigate models where α_D^a differs from α_D^c. We summarize these simulations below:

- We vary α_D as a constant value (Eq. 2), Section 5.1.

https://doi.org/10.5194/acp-2022-733
Preprint. Discussion started: 23 November 2022


Atmospheric Chemistry and Physics Discussions

- We vary α_D assuming the updated temperature dependence of s_{crit} from (Harrington et al., 2019), and investigate different surface growth mechanisms (Figure 2), Section 5.2.

- We vary α_D assuming dislocation growth (m=1), under the assumption of various temperature dependent parameterizations for s_{crit} (Figure 3), Section 5.2.

Simulations of experiments performed in the same temperature range and with the same IN demonstrated similar biases with respect to these models. We discuss detailed comparisons of models and observations below.

5.1 Sensitivity to surface kinetic effects (α_D = Const.)

We first investigated the average efficiency of ice growth by comparing with different constant values for α_D to see if ensemble ice growth in these conditions can in general be modeled with a constant deposition coefficient, as was assumed in Skrotzki et al. (2013) and has been a typical assumption used in cloud models. By running the parcel model with α_D values of 1.0, 0.2, 0.1, 0.01, and 0.001, we investigated the dependence of the ice growth rates on the deposition coefficient.

Figure 5 shows examples of the parcel model results for 3 experiments performed using ATD to nucleate ice heterogeneously across a range of temperatures (Exp. 4, $T = 230$ K, left column; Exp. 15, $T = 210$ K, middle column; and Exp. 21, $T = 190$ K, right column). The top three panels in each column are the observed temperature, pressure, and ice number concentration, which are used as inputs to the parcel model (the portion of the experiment that is modeled is shown as a red dashed line in each case). The fourth and fifth panels in each column are observed IWC and S_i, respectively, vs. the model results under different assumptions for a constant deposition coefficient. The sixth panel shows the time-dependent value of the deposition coefficient for each simulation (in this case, it is constant while ice is present). In general, the parcel model assuming a constant deposition coefficient agreed best with observations at higher temperatures, and demonstrated the most significant deviations at lower temperatures (< 205 K). Experiments at 235 K (Exp. 1-5) could be consistently modeled with a constant deposition coefficient. Experiments at 224 K (Exp. 7-11) also showed very good agreement with the exception of the initial nucleation phase, where IWC was generally underestimated, and S_i was overestimated by the model. We quantify this further in Section 5.4.

During Exp. 4, there were two separate changes in pressure (from approximately 0-250 s and again from 300 - 750 s in the left panel of Fig. 5), which allowed some of the ice to initially sublimate and then regrow. The modeled IWC and S_i agree well with the higher deposition coefficient models across both the phases of the experiment, indicating that depositional growth and evaporation can be modeled consistently in these conditions. Exp. 4, similar to a significant fraction of the higher temperature experiments (> 220 K) with heterogeneous nucleation on ATD, showed very little sensitivity to α_D for values > 0.2.

Exp. 15 is an illustrative example of an experiment at 210 K with ice growth by heterogeneous nucleation on ATD; these experiments (Exp. 12-17) generally showed good agreement with the model, although the IWC is overestimated by models with α_D for values > 0.2, even though S_i is consistent with the observations, particularly for $\alpha_D = 1$.

Exp. 21 demonstrates the greater deviation of the model from the observations at lower temperatures; similar behavior is observed in the other experiments with ATD at these temperatures (Exp. 20, 22, 32, and 33). Assuming $\alpha_D = 1$ actually results

https://doi.org/10.5194/acp-2022-733
Preprint. Discussion started: 23 November 2022

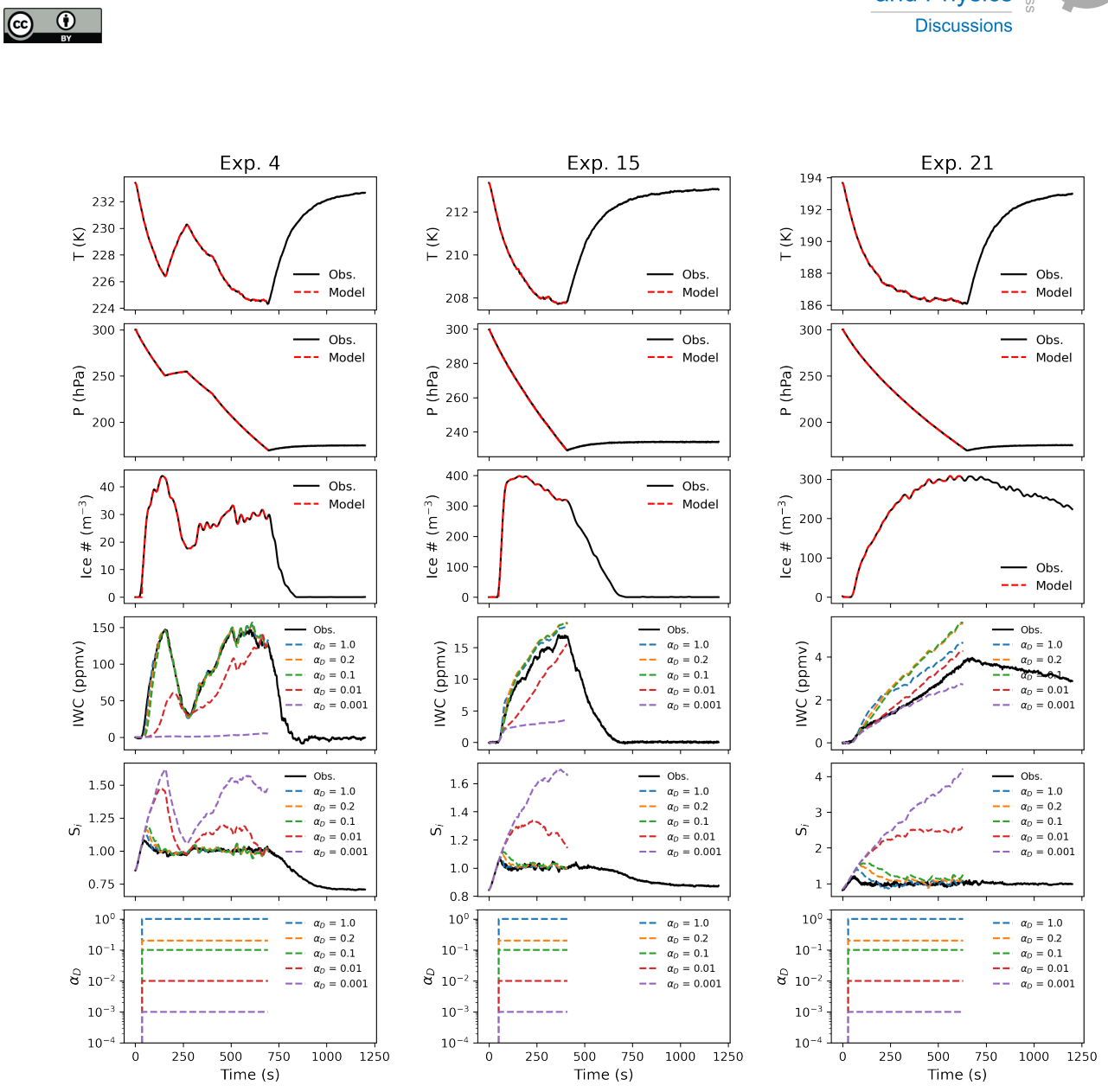

Figure 5. Parcel model results for different constant values of α_D. Three experiments are shown with different values for constant α_D, across a range of temperatures. The modeled IWC in experiment 4 ($T = 230$ K, ATD) is very insensitive to the value for α_D except during the initial nucleation phase. Experiment 15 ($T = 210$ K, ATD) also demonstrates very efficient ice growth, but the modeled IWC shows more significant deviations from the model for $\alpha_D > 0.1$. Experiment 21 ($T = 194$ K, ATD) indicates a case where the IWC is best fit by a constant α_D less than 1; however the observed S_i would not be consistent with the model in this case.

in lower IWC in some cases than smaller values of α_D (e.g. for Exp. 21, the blue vs green and yellow lines in the fourth panel of the right column in Figure 5), as the very efficient growth depleted the available vapor too quickly, bringing the vapor pressure below saturation and leading to a lower IWC after 200s.

https://doi.org/10.5194/acp-2022-733
Preprint. Discussion started: 23 November 2022

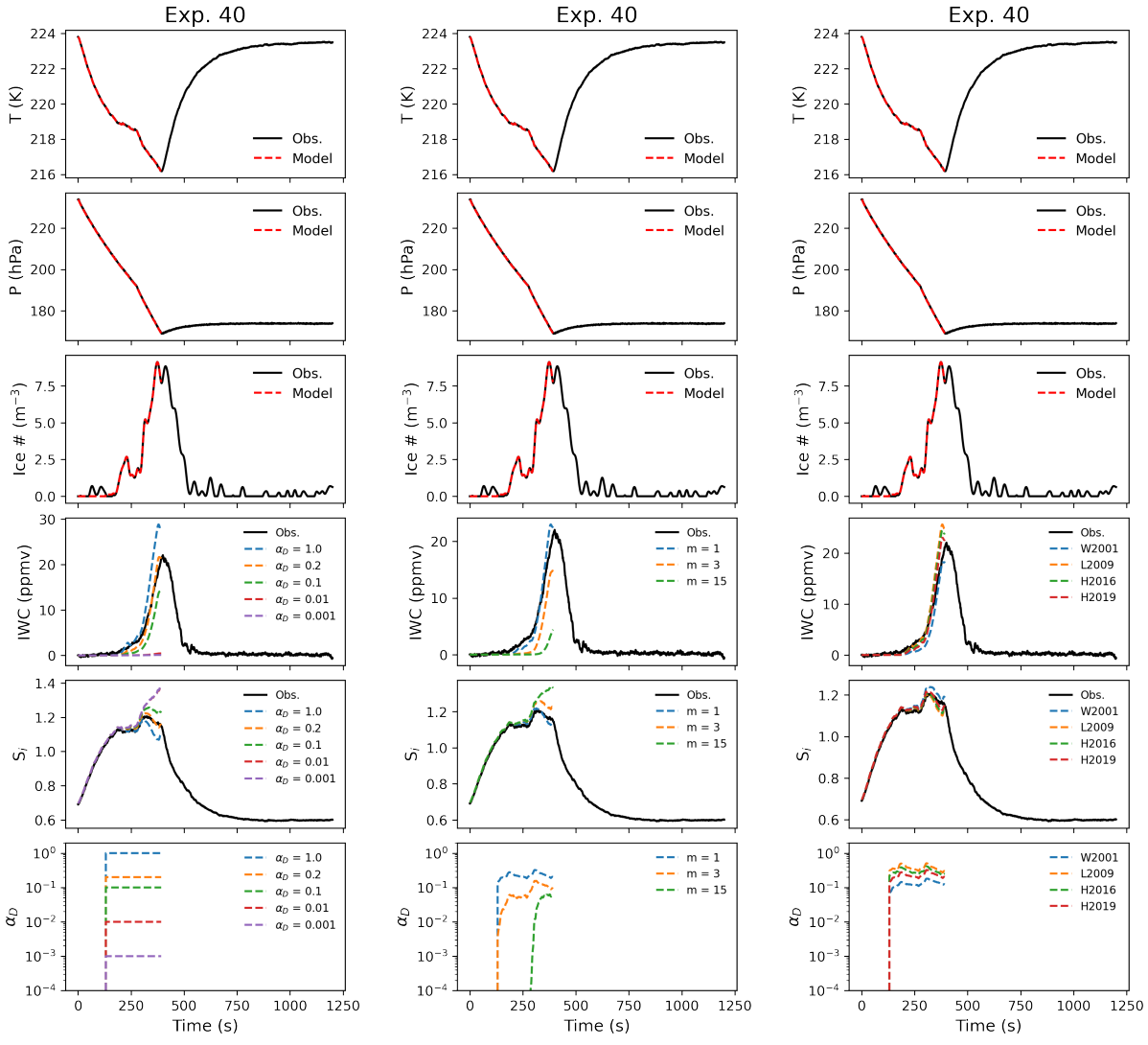

Figure 6. Comparison between deposition models. For experiment 40, we show parcel model output for IWC and S_i for different constant values of α_D (left), and for different ice surfaces (middle, varying m in Eq. 3), and for different parameterizations of s_{crit} (right, assuming $m = 1$ in Eq. 3). The top panel in each column shows the temperature and pressure, the second panel the ice water content (as equivalent water vapor mixing ratio), the third panel the ice number concentration, the 4th panel the supersaturation with respect to ice, and the bottom panel the values for α_D in each case. The value for s_{crit} for the model results shown in the middle column is derived from the temperature dependence measured in (Harrington et al., 2019).

https://doi.org/10.5194/acp-2022-733
Preprint. Discussion started: 23 November 2022

Atmospheric Chemistry and Physics Discussions

5.2 Modeling deposition coefficient with parameterization from Nelson and Baker, 1996

We also investigated ice growth with a deposition coefficient parameterized in terms of a temperature dependent critical supersaturation (Eq. 3), under the assumption of various growth mechanisms. In addition to uncertainty about the surface growth mechanism (m in Eq. 3), the temperature dependent critical supersaturation at temperatures below 233 K is not known. Previous measurements of critical supersaturations for basal and prism facets have been limited to higher temperatures (Nelson and Knight, 1998; Libbrecht and Rickerby, 2013; Harrison et al., 2016; Harrington et al., 2019). Growth rates and habits for ice at temperatures between 203 K and 253 K were experimentally measured in (Bailey and Hallett, 2004). Even at warmer temperatures, these measurements have significant discrepancies between them, however (See Figure 3), and the functional form for the critical supersaturation at colder temperatures is not known, as there is not yet consensus about the theoretical basis for this critical supersaturation (Burton et al., 1951; Libbrecht, 2005). The theoretical values are generally derived for the case of ice formation from pure water vapor, although chemical impurities and the existence of quasi-disordered layers could also significantly impact these values (Libbrecht, 2005). The mean displacement of molecules on the surface of a crystal is expected to increase at low temperatures, which means that s_{crit} should generally be inversely correlated with temperature (Burton et al., 1951).

We thus investigate the sensitivity of ice growth in AIDA to the surface growth mechanism by varying m (e.g. dislocation growth as $m = 1$, stacking fault dominated growth as $m = 3$, and 2D ledge nucleation as $m = 15$) and by using different parameterizations for the temperature dependence of s_{crit}. Figure 6 shows a comparison between observations and models for Exp. 40 ($T = 220$ K, ATD), for a constant deposition coefficient (left column), different assumptions for surface growth mechanisms (middle column), and different parameterizations for s_{crit} assuming dislocation growth ($m = 1$, right panel). When varying the surface growth mechanisms (middle column), we assume the temperature dependence of s_{crit} derived from Harrington et al. (2019), as experiments were generally most consistent with the lower values of the temperature dependence of the critical supersaturation (as will be discussed in Section 5.4). Exp. 40 had relatively low concentrations of IN present (Table 2).

Exp. 40 was best modeled by a constant deposition coefficient less than 1 ($\alpha_D = 0.2$), Figure 6 left column, fourth and fifth panels. This is similar to the value for α_D predicted for the experiment by Eq. 3, under the assumption of dislocation growth (Figure 6 middle column, sixth panel). The model also demonstrates some sensitivity to the temperature dependence of s_{crit} (assuming $m = 1$, Figure 6, right column), with the parameterizations predicting a lower temperature trend more closely matching the observed S_i and IWC. These simulations also indicate that ice growth during the initial phase of the experiment is more sensitive to the growth mechanism, while later ice growth is more sensitive to the temperature dependence of s_{crit}. Assuming ledge nucleation ($m = 15$) led to an initially very low deposition coefficient, which causes a significant increase in the simulated S_i in the latter part of the experiment when comparing against the simulations which assumed other surface growth mechanisms.

https://doi.org/10.5194/acp-2022-733
Preprint. Discussion started: 23 November 2022

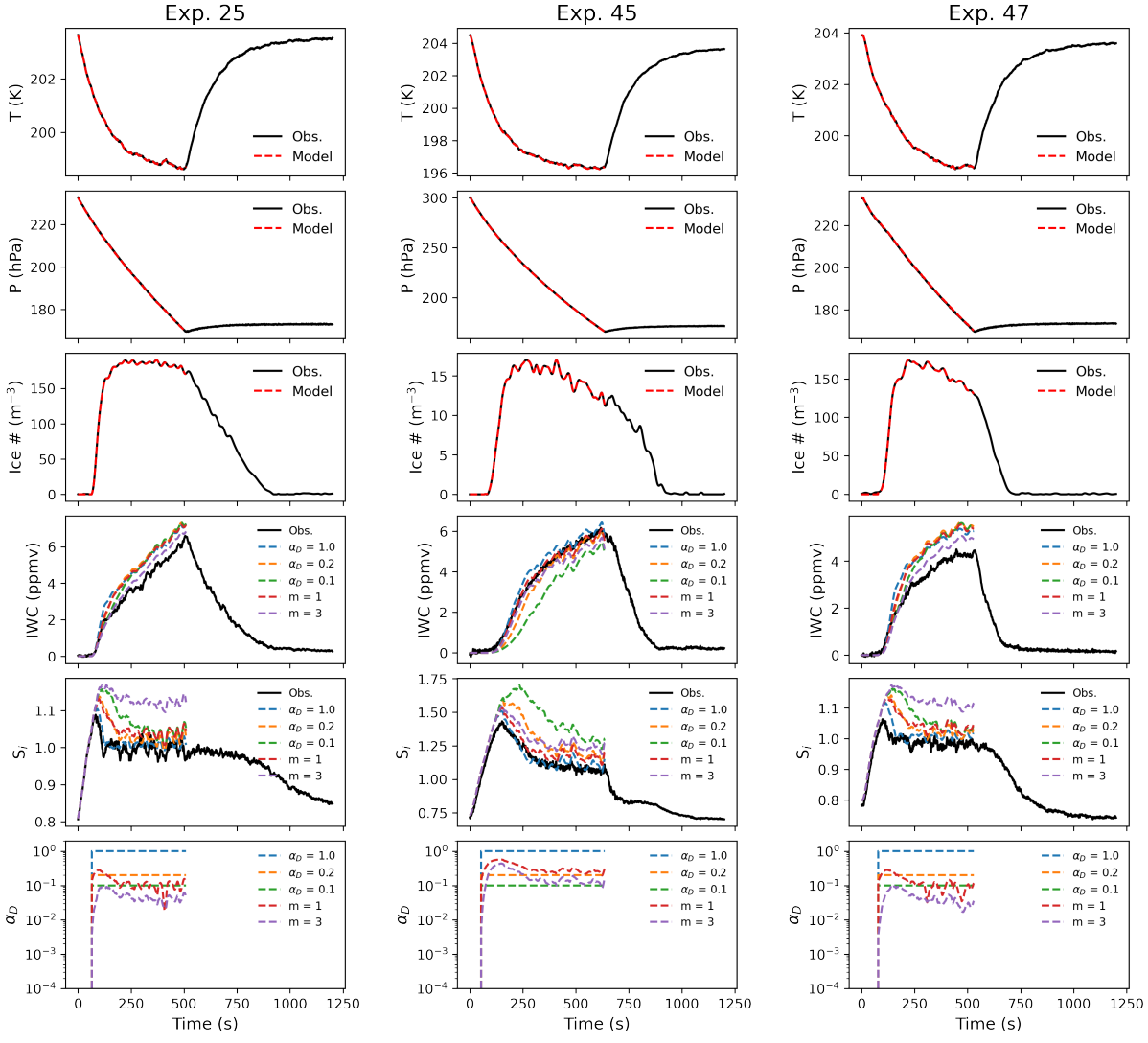

Figure 7. Comparison between deposition models for experiments at T = 205 K with different IN. Parcel model output for IWC and S_i for different values of α_D assuming different constant values (1.0, 0.2, or 0.1) or different ice surface growth mechanisms ($m = 1$ or $m = 3$) in Eq. 3. All three experiments took place at similar temperatures, but with different IN: Exp. 25 (ATD), Exp. 45 (SA), and Exp. 47 (ATD+SA).

5.3 Heterogeneous and homogeneous nucleation for experiments at T $\leq$ 205 K

385 We next compare experiments at 205 K that had different nucleation pathways. Exp. 24-27 were at 204 K and ice was formed through heterogeneous nucleation on ATD. Exp. 45 was at 205 K, and was a homogeneous nucleation experiment using SA. Exp. 46-48 had a mixture of both ATD and SA as IN. The homogeneous nucleation experiment (Exp. 45) could be

https://doi.org/10.5194/acp-2022-733
Preprint. Discussion started: 23 November 2022


Atmospheric Chemistry and Physics Discussions

consistently fit with a deposition coefficient near unity or with α_D as given by Eq. 3, assuming $m = 1$ (Figure 7, middle column), whereas the other experiments with heterogeneous IN produced lower IWC than would be predicted by the constant α_D models (α_D>0.1) or by Eq. 3 assuming dislocation growth. The IWC as predicted by Eq. 3 for Exp. 25 and Exp. 47 assuming $m = 3$ is closer to the observed IWC, but this model would predict significantly higher S_i than was observed in both experiments. Although Exp. 47 included both ATD and SA as IN, this result suggests that the ice growth is mainly controlled by the presence of the heterogeneous IN.

The difference between the heterogeneous and homogeneous nucleation experiments is consistent with the picture that subsequent ice growth in the atmosphere may be strongly influenced by the initial nucleation pathway. During Exp. 45, ice mainly grows in highly supersaturated conditions (Figure 7, middle column, fifth panel). Thus, ice growth should not be strongly limited by surface impedance in this case, as the high supersaturation required to nucleate ice in the homogeneous nucleation experiment leads to very efficient growth.

This effect could be enhanced by differences in ice surface growth mechanisms, as previous observations of surface complexity in AIDA indicate differences between experiments initiated with heterogeneous or homogeneous ice nucleating particles (Schnaiter et al., 2016; Järvinen et al., 2018). In addition, the growth mechanism may change as ice crystals grow or the environmental conditions change. Small ice detector probe (SID-3) measurements of ice formed at 223 K via homogeneous nucleation in AIDA demonstrated high complexity for these ice crystals; heterogeneous nucleation however was observed to lead to pristine ice (in the case of low supersaturation) and more complex ice for higher supersaturations (Schnaiter et al., 2016; Järvinen et al., 2018). This suggests that more complex ice in these conditions should be more likely to lead to growth by abundant surface dislocations.

Comparisons with experiments at lower temperatures ($T = 192$ K) with different IN (Figure 8) demonstrate similar results as those at $T = 205$ K (Figure 7). In this case, Exp. 20 was a heterogeneous nucleation experiment with ATD, Exp. 31 was a homogeneous nucleation experiment using SA, and Exp. 33 used a mix of ATD and SA. Similar to the experiments near 205 K, the homogeneous nucleation experiment could be fit relatively consistently with the constant deposition coefficient model assuming $\alpha_D = 1$ or Eq. 3 assuming dislocation growth. Both experiments with heterogeneous IN show a significant mismatch between all models and observations for both S_i and IWC. Varying the temperature dependence of s_{crit} could account for some of the discrepancy between the model and observations, but this result also may be enhanced by an underestimation of the total ice number density for the heterogeneous IN experiments at low temperatures (Clouser et al., 2020). These experiments generally had ice crystals with average radii very near the detection limit of the optical particle counters, and smaller ice crystals on average than were observed for the homogeneous nucleation experiments (Tables 1 and 2). Although both models used in Skrotzki et al. (2013) relied on different experimental observables, they also both used the ice number density as a model input, suggesting that the same systematic uncertainty related to undercounting ice at low temperatures would impact those results as well.

https://doi.org/10.5194/acp-2022-733
Preprint. Discussion started: 23 November 2022

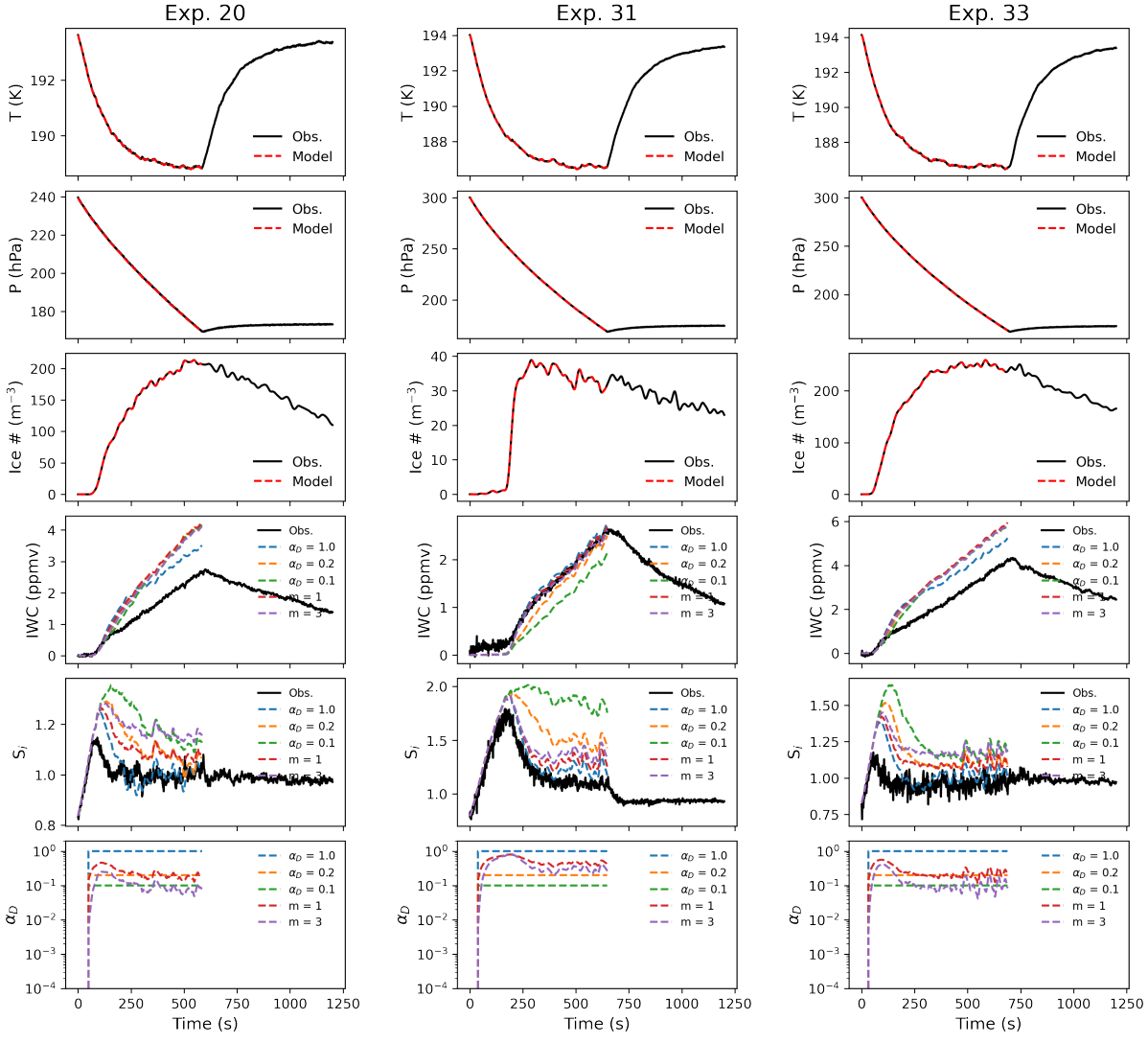

Figure 8. Comparison between deposition models for cold temperature experiments with different IN. Parcel model output for IWC and S_i for different values of α_s assuming different ice surface growth mechanisms in Eq. 3. All three experiments took place at similar temperatures, but with different IN: Exp. 20 (ATD), Exp. 31 (SA), and Exp. 33 (ATD+SA).

5.4 Comparison of models and observations as a function of temperature

To evaluate how the model predictions for S_i and IWC for the different simulations compare against the observed time series across all experiments, here we use Mean Absolute Percentage Error (MAPE). We adopt notation to define the observed time

https://doi.org/10.5194/acp-2022-733
Preprint. Discussion started: 23 November 2022


Atmospheric Chemistry and Physics Discussions

series for each experiment (either IWC or S_i) as y_i, and the model prediction as $\hat{y}_i$. MAPE is defined as

$$\text{MAPE} = \frac{1}{n}\sum_{i=1}^{n}\left|\frac{y_i - \hat{y}_i}{y_i} * 100\right| \tag{5}$$

where the summation is over the n modeled time steps. Because this metric is scale-independent, it can be used to compare model performance across different experiments. Lower values of MAPE indicate that observations and models more closely agree.

Figure 9 shows the MAPE as a function of temperature for S_i and IWC for the three sets of simulations. The most significant deviations between all models and observations occur below 205 K. For the constant α_D models (Figure 9a,b), the MAPE was generally smallest for α_D>0.2 for S_i across the entire temperature range, and for IWC above 205 K; below 205 K, the MAPE for IWC for some experiments was lower for α_D<0.1.

For the MAPE of S_i and IWC assuming α_D parameterized according to Eq. 3 with different surface growth mechanisms (Figure 9c,d), the experiments above 205 K had the smallest MAPE for both IWC and S_i assuming $m = 1$, or growth by abundant surface dislocations. For experiments below 205 K, the trend was less clear.

Under the assumption of dislocation growth (Figure 9e,f), MAPE for S_i was lower for the assumption that s_{crit} has a lower value at cold temperatures (Figure 3). We plan to further explore constraints placed on the parameterizations for s_{crit} by these experiments in future work.

To explain why many experiments are consistent with both Eq. 2 and Eq. 3, we note that the radius of the ice crystals only change by a single order of magnitude over the course of these experiments (in most cases from ∼1 to ∼5-10μm). This small range of values, coupled with dislocation growth, means that the deposition coefficient is relatively constant over the experiment. In Exp. 40 for example, the deposition coefficient in the dislocation model ranges from ∼1 to 0.1, which is also a range over which the model is quite insensitive to the deposition coefficient in the constant case (Figure 6).

6 Conclusions

Previous experiments in AIDA indicated that the deposition coefficient was within an order of magnitude of unity in cirrus conditions. However, these experiments only considered a model where the deposition coefficient was constant, and these values should be interpreted as an average over the evolving environmental conditions during the expansion experiments. Here we have shown that even though ice growth in cold cloud experiments in AIDA can be modeled with a constant deposition coefficient in most cases, it is also consistent with models of surface kinetic effects that vary as a function of supersaturation and temperature.

Even though these expansion experiments did not generally demonstrate significant depositional growth inhibition due to these surface kinetic effects, we recommend caution in extrapolating from these experiments to real atmospheric conditions. Cloud chamber expansion experiments involve much more rapid changes in supersaturation, temperature, and pressure than are generally found in the atmosphere, and experiments at colder temperatures (< 205 K) demonstrated greater sensitivity to the deposition parameterization, and more significant deviations from all depositional growth models (See Figure 9). Ice

https://doi.org/10.5194/acp-2022-733
Preprint. Discussion started: 23 November 2022

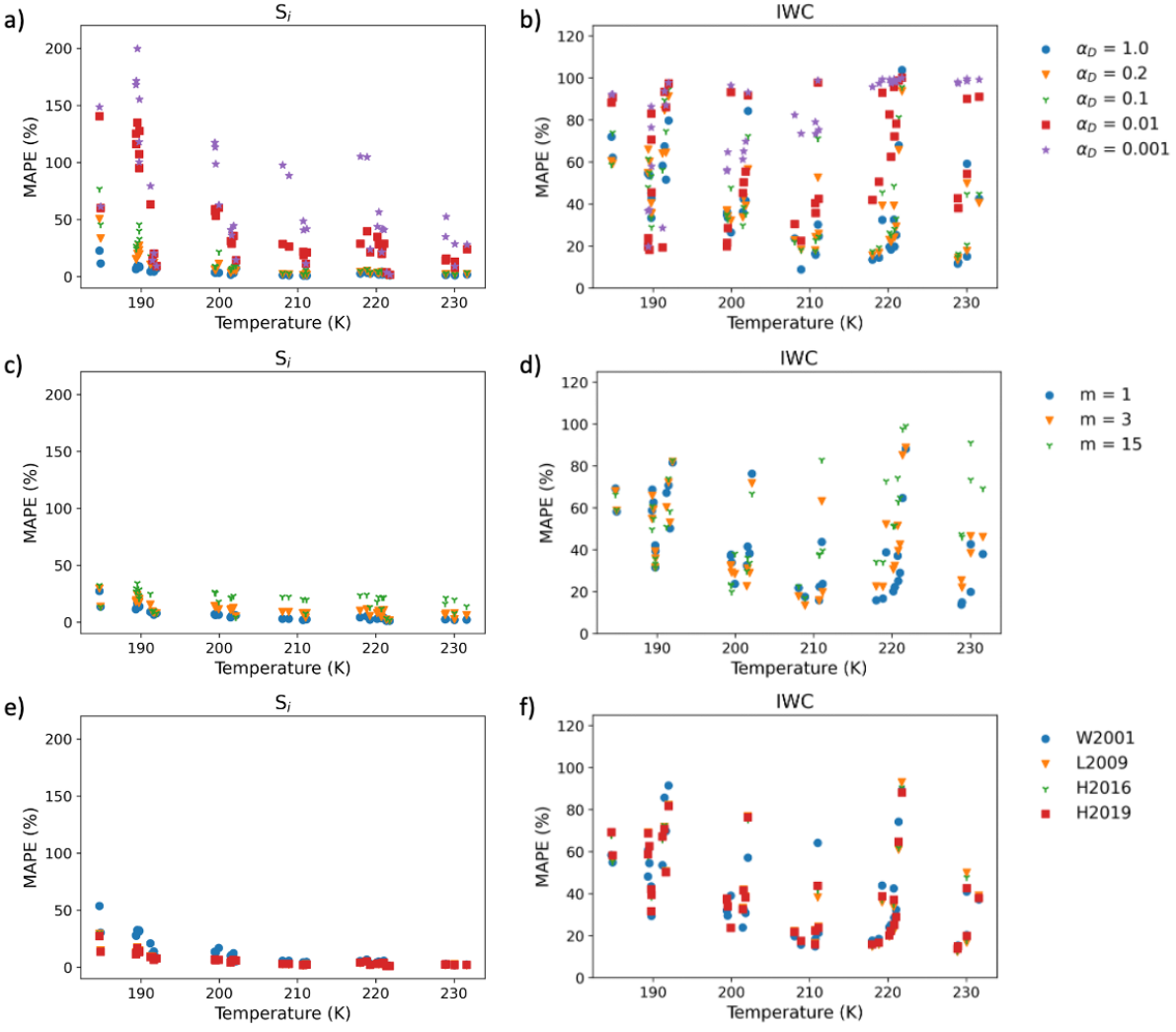

Figure 9. Mean absolute percentage error for deposition models. (a,b) Temperature dependence of MAPES for IWC and S_i for the constant α_D models for all the IsoCloud experiments. (c,d) For the different surface growth mechanisms. (e,g) For different temperature parameterizations for s_{crit} assuming $m = 1$ in Eq. 3. Here we use the following abbreviations in the legend: W2001 (Wood et al., 2001); L2009 (Libbrecht and Arnold, 2009), H2016 (Harrison et al., 2016), and H2019 (Harrington et al., 2019)

455 growth in AIDA occurs at significantly higher effective updraft speeds (90-370 cm/s for the IsoCloud experiments) than are present in atmospheric cirrus clouds forming in the tropical tropopause layer, where updraft speeds are generally a few cm/s (Krämer et al., 2020). In addition, since populations of ice crystals within AIDA nucleate and grow in relatively consistent conditions, they may not represent the true heterogeneity of ice crystal populations growing in competition with one another in atmospheric conditions. Since surface kinetic effects will be most significant for ice growth from vapor near saturation, 460 the much lower updraft speeds found in regions where atmospheric cirrus form indicate these surface kinetic effects should

https://doi.org/10.5194/acp-2022-733
Preprint. Discussion started: 23 November 2022


Atmospheric Chemistry and Physics Discussions

not be neglected in cloud models. (However, these results may be more representative of specific atmospheric conditions with significantly higher updraft speeds, such as cirrus clouds formed as the result of overshooting convective systems or in systems with large scale updrafts such as the Asian monsoon (Krämer et al., 2020)).

These results also demonstrate that the seeming contradiction between the high deposition coefficients previously observed in cloud chamber experiments (Skrotzki et al., 2013) and the low deposition coefficients observed in single particle levitation diffusion chamber experiments (Magee et al., 2006) can be resolved by a non-constant parameterization for α_D. Here we have shown that both types of experiments can be consistently modeled with the same ice growth theory. Although the AIDA experiments can in some cases be fit with a constant deposition coefficient, the value of the deposition coefficient cannot be predicted directly based on other environmental observables, such as saturation, temperature, and pressure (as the s_{crit} model in Eq. 3 can be). In a general sense, when α_D is greater than 0.1, attachment kinetics can usually be ignored in mass growth estimates, while $\alpha_D < 0.1$ produces effects on growth that generally cannot be ignored. However, the deposition coefficient in both limits must be included in order to consistently model changes in crystal shape. These results suggest that chamber experiments should not be over-interpreted to imply that the deposition coefficient will always be unimportant for cirrus formation.

Ice growth at low temperatures may also be further complicated by a metastable cubic ice phase (I_c), which laboratory studies and molecular dynamic simulations have indicated could exist in atmospheric conditions at low temperatures (Murray et al., 2005). Molecular dynamics simulations at 180 K indicated additional complications for crystal surfaces at low temperatures, including the aggregation of I_h and I_c to form poly-crystals, leading to stacking faults and random grain boundaries (2-dimensional crystal defects) (Moore and Molinero, 2011a, b). Ice crystals with three-fold symmetry (trigonal ice) have also been observed in the atmosphere, and have been related to stacking disorders in the ice crystal lattice (Murray et al., 2015). A recent study exploring experimental water vapor pressure measurements for amorphous solid water and supercooled liquid water crystallizing below 235 K suggests these two distinct phases of water may have a phase transition between 200 K and 235 K, which could help explain high supersaturations observed in the TTL (Nachbar et al., 2019). We have not explored these issues here, but they may be important processes in certain atmospheric conditions, and are discussed in the context of the IsoCloud experiments in Clouser et al. (2020).

The IsoCloud experiments provided observational constraints on the values for the critical supersaturation at low temperatures. These experiments indicate that homogeneous nucleation and heterogeneous nucleation in cases of high supersaturation can generally be parameterized as dislocation growth consistent with a temperature dependent critical supersaturation; however ice clouds forming in the atmosphere via heterogeneous nucleation at low ambient supersaturations could proceed via growth mechanisms with a stronger dependence on critical supersaturation (i.e. m>1 in Eq. 3). Additionally, changing conditions of supersaturations have previously been indicated as a mechanism for lower growth rates, even when ice was initially nucleated homogeneously (Zhang and Harrington, 2014). More precise laboratory experiments are needed to constrain the distinct growth rates of the basal and prism facets at low temperatures, as the analysis presented here provides only an average growth rate (dominated by growth on the principal facet). These experiments suggest that both nucleation pathway (homogeneous or heterogeneous) and ice number density (low or high) may lead to different surface effects. In a follow up paper (Part 2) we

https://doi.org/10.5194/acp-2022-733
Preprint. Discussion started: 23 November 2022

will apply Bayesian parameter estimation to more qualitatively evaluate the constraints placed on depositional growth models by the AIDA experiments.

Code and data availability. IsoCloud experiment data and python code to preprocess and analyze experiments is available at https://github.com/kdlamb/isc The Lagrangian parcel model code used in this analysis was provided by J.Y. Harrington.

Competing interests. Two of the co-authors (Harald Saathoff and Ottmar Möhler) are members of the editorial board of ACP. The peer-review process was guided by an independent editor, and the authors also have no other competing interests to declare.

Acknowledgements. The authors acknowledge support from the U.S. Department of Energy's Atmospheric Science Program Atmospheric System Research, an Office of Science, Office of Biological and Environmental Research program under grant DE-SC0023020. J.Y. Harrington is grateful for support from the National Science Foundation, grant AGS-2128347, and the U.S. Department of Energy's Atmospheric Science Program Atmospheric System Research, an Office of Science, Office of Biological and Environmental Research program under grant DE-SC0021001. We also acknowledge the IsoCloud science team and the AIDA technical staff and support team. Funding for the IsoCloud campaign was provided by the National Science Foundation (NSF) and the Deutsche Forschungsgemeinschaft through International Collaboration in Chemistry grants CHEM1026830 and MO 668/3-1.

https://doi.org/10.5194/acp-2022-733
Preprint. Discussion started: 23 November 2022

Atmospheric Chemistry and Physics Discussions

References

Bailey, M. and Hallett, J.: Nucleation effects on the habit of vapour grown ice crystals from- 18 to- 42 C, Quarterly Journal of the Royal Meteorological Society, 128, 1461–1483, https://doi.org/10.1002/qj.200212858 304, 2002.

Bailey, M. and Hallett, J.: Growth rates and habits of ice crystals between- 20 and- 70 C, Journal of the Atmospheric Sciences, 61, 514–544, https://doi.org/10.1175/1520–0469(2004)061<0514:GRAHOI>2.0.CO;2, 2004.

Bailey, M. and Hallett, J.: Ice crystal linear growth rates from- 20 to- 70 C: Confirmation from wave cloud studies, Journal of the Atmospheric Sciences, 69, 390–402, https://doi.org/10.1175/JAS–D–11–035.1, 2012.

Bailey, M. P. and Hallett, J.: A comprehensive habit diagram for atmospheric ice crystals: Confirmation from the laboratory, AIRS II, and other field studies, Journal of the Atmospheric Sciences, 66, 2888–2899, DOI:10.1175/2009JAS2883.1, 2009.

Benz, S., Megahed, K., Möhler, O., Saathoff, H., Wagner, R., and Schurath, U.: T-dependent rate measurements of homogeneous ice nucleation in cloud droplets using a large atmospheric simulation chamber, Journal of Photochemistry and Photobiology A: Chemistry, 176, 208–217, https://doi.org/10.1016/j.jphotochem.2005.08.026, 2005.

Burton, W.-K., Cabrera, N., and Frank, F.: The growth of crystals and the equilibrium structure of their surfaces, Phil. Trans. R. Soc. Lond. A, 243, 299–358, DOI:10.1098/rsta.1951.0006, 1951.

Clouser, B. W., Lamb, K. D., Sarkozy, L. C., Habig, J., Ebert, V., Saathoff, H., Möhler, O., and Moyer, E. J.: No anomalous supersaturation in ultracold cirrus laboratory experiments, Atmospheric Chemistry and Physics, 20, 1089–1103, https://doi.org/10.5194/acp-20-1089-2020, 2020.

Cotton, R., Benz, S., Field, P., Möhler, O., and Schnaiter, M.: A numerical test-bed for detailed ice nucleation studies in the AIDA cloud simulation chamber, Atmospheric Chemistry and Physics, 7, 243–256, DOI:10.5194/ACP–7–243–2007, 2007.

Dinh, T., Podglajen, A., Hertzog, A., Legras, B., and Plougonven, R.: Effect of gravity wave temperature fluctuations on homogeneous ice nucleation in the tropical tropopause layer, Atmospheric Chemistry and Physics, 16, 35–46, DOI:10.5194/ACP–16–35–2016, 2016.

Fahey, D. W., Gao, R.-S., Möhler, O., Saathoff, H., Schiller, C., Ebert, V., Krämer, M., Peter, T., Amarouche, N., Avallone, L. M., Bauer, R., Bozóki, Z., Christensen, L. E., Davis, S. M., Durry, G., Dyroff, C., Herman, R. L., Hunsmann, S., Khaykin, S. M., Mackrodt, P., Meyer, J., Smith, J. B., Spelten, N., Troy, R. F., Vömel, H., Wagner, S., and Wienhold, F. G.: The AquaVIT-1 intercomparison of atmospheric water vapor measurement techniques, Atmospheric Measurement Techniques, 7, 3177–3213, https://doi.org/10.5194/amt-7-3177-2014, 2014.

Gao, R., Popp, P., Fahey, D., Marcy, T., Herman, R., Weinstock, E., Baumgardner, D., Garrett, T., Rosenlof, K., Thompson, T., et al.: Evidence that nitric acid increases relative humidity in low-temperature cirrus clouds, Science, 303, 516–520, DOI:10.1126/SCIENCE.1091 255, 2004.

Gao, R.-S., Gierczak, T., Thornberry, T. D., Rollins, A. W., Burkholder, J. B., Telg, H., Voigt, C., Peter, T., and Fahey, D. W.: Persistent Water–Nitric Acid Condensate with Saturation Water Vapor Pressure Greater than That of Hexagonal Ice, The Journal of Physical Chemistry A, 120, 1431–1440, DOI:10.1021/acs.jpca.5b06 357, 2015.

Gierens, K. M., Monier, M., and Gayet, J.-F.: The deposition coefficient and its role for cirrus clouds, Journal of Geophysical Research: Atmospheres, 108, DOI:10.1029/2001JD001 558, 2003.

Hallett, J. and Mason, B. J.: The influence of temperature and supersaturation on the habit of ice crystals grown from the vapour, Proc. R. Soc. Lond. A, 247, 440–453, DOI:10.1098/rspa.1958.0199, 1958.

Harrington, J. Y. and Pokrifka, G. F.: Approximate Models for Lateral Growth on Ice Crystal Surfaces during Vapor Depositional Growth, Journal of the Atmospheric Sciences, 78, 967–981, DOI:10.1175/jas–d–20–0228.1, 2021.

https://doi.org/10.5194/acp-2022-733
Preprint. Discussion started: 23 November 2022

Atmospheric Chemistry and Physics Discussions

Harrington, J. Y., Moyle, A., Hanson, L. E., and Morrison, H.: On Calculating Deposition Coefficients and Aspect-Ratio Evolution in Approximate Models of Ice Crystal Vapor Growth, Journal of the Atmospheric Sciences, 76, 1609–1625, DOI:10.1175/JAS–D–18–0319.1, https://doi.org/10.1175/JAS-D-18-0319.1, 2019.

Harrison, A., Moyle, A. M., Hanson, M., and Harrington, J. Y.: Levitation Diffusion Chamber Measurements of the Mass Growth of Small Ice Crystals from Vapor, Journal of the Atmospheric Sciences, 73, 2743–2758, DOI:10.1175/JAS–D–15–0234.1, 2016.

Hiranuma, N., Hoffmann, N., Kiselev, A., Dreyer, A., Zhang, K., Kulkarni, G., Koop, T., and Möhler, O.: Influence of surface morphology on the immersion mode ice nucleation efficiency of hematite particles, Atmospheric Chemistry and Physics, 14, 2315–2324, DOI:10.5194/ACP–14–13 145–2014, 2014a.

Hiranuma, N., Paukert, M., Steinke, I., Zhang, K., Kulkarni, G., Hoose, C., Schnaiter, M., Saathoff, H., and Möhler, O.: A comprehensive parameterization of heterogeneous ice nucleation of dust surrogate: laboratory study with hematite particles and its application to atmospheric models, Atmospheric Chemistry and Physics, 14, 13 145–13 158, DOI:10.5194/ACP–14–2315–2014, 2014b.

Järvinen, E., Jourdan, O., Neubauer, D., Yao, B., Liu, C., Andreae, M. O., Lohmann, U., Wendisch, M., McFarquhar, G. M., Leisner, T., et al.: Additional global climate cooling by clouds due to ice crystal complexity, Atmospheric Chemistry and Physics, 18, 15 767–15 781, DOI:10.5194/ACP–18–15 767–2018, 2018.

Jensen, E. J., Ueyama, R., Pfister, L., Bui, T. V., Alexander, M. J., Podglajen, A., Hertzog, A., Woods, S., Lawson, R. P., Kim, J.-E., et al.: High-frequency gravity waves and homogeneous ice nucleation in tropical tropopause layer cirrus, Geophysical Research Letters, 43, 6629–6635, DOI:10.1002/2016GL069 426, 2016.

Kaufmann, S., Voigt, C., Heller, R., Jurkat-Witschas, T., Krämer, M., Rolf, C., Zöger, M., Giez, A., Buchholz, B., Ebert, V., Thornberry, T., and Schumann, U.: Intercomparison of midlatitude tropospheric and lower-stratospheric water vapor measurements and comparison to ECMWF humidity data, Atmospheric Chemistry and Physics, 18, 16 729–16 745, DOI:10.5194/ACP–18–16 729–2018, https://doi.org/10.5194/acp-18-16729-2018, 2018.

Kiselev, A., Bachmann, F., Pedevilla, P., Cox, S. J., Michaelides, A., Gerthsen, D., and Leisner, T.: Active sites in heterogeneous ice nucleation—the example of K-rich feldspars, Science, pp. aai8034, DOI:10.1126/science.aai8034, 2016.

Kong, X., Papagiannakopoulos, P., Thomson, E. S., Markovic, N., and Pettersson, J. B.: Water accommodation and desorption kinetics on ice, The Journal of Physical Chemistry A, 118, 3973–3979, DOI:10.1021/jp503 504e, 2014a.

Kong, X., Thomson, E. S., Papagiannakopoulos, P., Johansson, S. M., and Pettersson, J. B.: Water accommodation on ice and organic surfaces: Insights from environmental molecular beam experiments, The Journal of Physical Chemistry B, 118, 13 378–13 386, DOI:10.1021/jp5044 046, 2014b.

Koop, T., Luo, B., Tsias, A., and Peter, T.: Water activity as the determinant for homogeneous ice nucleation in aqueous solutions, Nature, 406, 611, DOI:10.1038/35020 537, 2000.

Krämer, M., Rolf, C., Spelten, N., Afchine, A., Fahey, D., Jensen, E., Khaykin, S., Kuhn, T., Lawson, P., Lykov, A., et al.: A microphysics guide to cirrus–Part 2: Climatologies of clouds and humidity from observations, Atmospheric chemistry and physics, 20, 12 569–12 608, DOI:10.5194/acp–2020–40, 2020.

Kuroda, T. and Lacmann, R.: Growth kinetics of ice from the vapour phase and its growth forms, Journal of Crystal Growth, 56, 189–205, DOI:10.1016/0022–0248(82)90 028–8, 1982.

Lamb, D. and Chen, J.-P.: An expanded parameterization of the growth of ice crystals by vapor deposition, in: Preprints, Conference on Cloud Physics, 75th AMS Annual Meeting, Jan 15-20, pp. 389–392, 1995.

https://doi.org/10.5194/acp-2022-733
Preprint. Discussion started: 23 November 2022

Atmospheric Chemistry and Physics Discussions

Lamb, D. and Scott, W. D.: The mechanism of ice crystal growth and habit formation, Journal of the atmospheric sciences, 31, 570–580, DOI:10.1175/1520–0469(1974)031<0570:TMOICG>2.0.CO;2, 1974.

Lamb, K. D., Clouser, B. W., Bolot, M., Sarkozy, L., Ebert, V., Saathoff, H., Möhler, O., and Moyer, E. J.: Laboratory measurements of HDO/H2O isotopic fractionation during ice deposition in simulated cirrus clouds, Proceedings of the National Academy of Sciences, 114, 5612–5617, DOI:10.1073/pnas.1618374 114, 2017.

Lauer, C.: Aufbau und Validierung eines kalibrationsfreien, extraktiven 1.4 um-Laserhygrometers für den Einsatz an der Aerosolkammer AIDA, Ph.D. thesis, PhD thesis, 2007.

Lewis, B.: The growth of crystals at low supersaturation: II. Comparison with experiment, Journal of Crystal Growth, 21, 40–50, 1974.

Libbrecht, K. and Arnold, H.: Measurements of ice crystal growth rates in air at-5C and-10C, arXiv preprint arXiv:0912.2518, 2009.

Libbrecht, K. G.: Explaining the formation of thin ice crystal plates with structure-dependent attachment kinetics, Journal of Crystal Growth, 258, 168–175, DOI:10.1016/S0022–0248(03)01 496–9, 2003.

Libbrecht, K. G.: A critical look at ice crystal growth data, arXiv preprint cond-mat/0411662, 2004.

Libbrecht, K. G.: The physics of snow crystals, Reports on progress in physics, 68, 855, DOI:10.1088/0034–4885/68/4/R03, 2005.

Libbrecht, K. G. and Rickerby, M. E.: Measurements of surface attachment kinetics for faceted ice crystal growth, Journal of Crystal Growth, 377, 1–8, DOI:10.1016/J.JCRYSGRO.2013.04.037, 2013.

Lin, R.-F., Starr, D. O., DeMott, P. J., Cotton, R., Sassen, K., Jensen, E., Kärcher, B., and Liu, X.: Cirrus parcel model comparison project. Phase 1: The critical components to simulate cirrus initiation explicitly, Journal of the Atmospheric Sciences, 59, 2305–2329, DOI:10.1175/1520–0469(2002)059<2305:cpmcpp>2.0.co;2, 2002.

Magee, N., Moyle, A. M., and Lamb, D.: Experimental determination of the deposition coefficient of small cirrus-like ice crystals near- 50 ° C, Geophysical Research Letters, 33, DOI:10.1029/2006GL026 665, 2006.

Magee, N., Boaggio, K., Staskiewicz, S., Lynn, A., Zhao, X., Tusay, N., Schuh, T., Bandamede, M., Bancroft, L., Connelly, D., Hurler, K., Miner, B., and Khoudary, E.: Captured cirrus ice particles in high definition, Atmospheric Chemistry and Physics, 21, 7171–7185, 10.5194/acp–21–7171–2021, https://doi.org/10.5194/acp-21-7171-2021, 2021.

Mason, B.: The Physics of Clouds, Clarendon Press, 1971.

Ming, N.-B., Tsukamoto, K., Sunagawa, I., and Chernov, A.: Stacking faults as self-perpetuating step sources, Journal of Crystal Growth, 91, 11–19, DOI:10.1016/0022–0248(88)90 360–0, 1988.

Möhler, O., Field, P., Connolly, P., Benz, S., Saathoff, H., Schnaiter, M., Wagner, R., Cotton, R., Krämer, M., Mangold, A., et al.: Efficiency of the deposition mode ice nucleation on mineral dust particles, Atmospheric Chemistry and Physics, 6, 3007–3021, DOI:10.5194/ACP–6–3007–2006, 2006.

Moore, E. B. and Molinero, V.: Is it cubic? Ice crystallization from deeply supercooled water, Physical Chemistry Chemical Physics, 13, 20 008–20 016, DOI:10.1039/c1cp22 022e, 2011a.

Moore, E. B. and Molinero, V.: Structural transformation in supercooled water controls the crystallization rate of ice, Nature, 479, 506, DOI:10.1038/nature10 586, 2011b.

Murray, B. J., Knopf, D. A., and Bertram, A. K.: The formation of cubic ice under conditions relevant to Earth's atmosphere, Nature, 434, 202, DOI:10.1038/nature03 403, 2005.

Murray, B. J., Salzmann, C. G., Heymsfield, A. J., Dobbie, S., Neely III, R. R., and Cox, C. J.: Trigonal ice crystals in Earth's atmosphere, Bulletin of the American Meteorological Society, 96, 1519–1531, DOI:10.1175/BAMS–D–13–00 128.1, 2015.

Nachbar, M., Duft, D., and Leisner, T.: The vapor pressure of liquid and solid water phases at conditions relevant to the atmosphere, The Journal of Chemical Physics, 151, 064 504, DOI:10.1063/1.5100 364, 2019.

Nelson, J.: Interactive comment on "Supersaturation, dehydration, and denitrification in Arctic cirrus" by B. Kärcher, Atmos. Chem. Phys. Discuss., 5, S257–S260, 2005.

Nelson, J. and Baker, M.: New theoretical framework for studies of vapor growth and sublimation of small ice crystals in the atmosphere, Journal of Geophysical Research: Atmospheres, 101, 7033–7047, DOI:10.1029/95JD03 162, 1996.

Nelson, J. and Knight, C.: Snow crystal habit changes explained by layer nucleation, Journal of the Atmospheric Sciences, 55, 1452–1465, DOI:10.1175/1520–0469(1998)055<1452:SCHCEB>2.0.CO;2, 1998.

Pokrifka, G. F., Moyle, A. M., Hanson, L. E., and Harrington, J. Y.: Estimating Surface Attachment Kinetic and Growth Transition Influences on Vapor-Grown Ice Crystals, Journal of the Atmospheric Sciences, 77, 2393–2410, DOI:10.1175/jas–d–19–0303.1, 2020.

Pratte, P., van den Bergh, H., and Rossi, M. J.: The kinetics of H2O vapor condensation and evaporation on different types of ice in the range 130- 210 K, The Journal of Physical Chemistry A, 110, 3042–3058, DOI:10.1021/JP053 974S, 2006.

Pruppacher, H. R., Klett, J. D., and Wang, P. K.: Microphysics of clouds and precipitation, 1998.

Randel, W. J. and Jensen, E. J.: Physical processes in the tropical tropopause layer and their roles in a changing climate, Nature Geoscience, 6, 169–176, DOI:10.1038/NGEO1733, 2013.

Sarkozy, L. C., Clouser, B. W., Lamb, K. D., Stutz, E. J., Saathoff, H., Moehler, O., Ebert, V., and Moyer, E. J.: The Chicago Water Isotope Spectrometer (ChiWIS-lab): A tunable diode laser spectrometer for chamber-based measurements of water vapor isotopic evolution during cirrus formation, Review of Scientific Instruments, 91, 045 120, https://doi.org/10.1063/1.5139244, 2020.

Sazaki, G., Zepeda, S., Nakatsubo, S., Yokoyama, E., and Furukawa, Y.: Elementary steps at the surface of ice crystals visualized by advanced optical microscopy, Proceedings of the National Academy of Sciences, p. DOI:10.1073/pnas.1008866107, 2010.

Sazaki, G., Asakawa, H., Nagashima, K., Nakatsubo, S., and Furukawa, Y.: Double spiral steps on Ih ice crystal surfaces grown from water vapor just below the melting point, Crystal Growth & Design, 14, 2133–2137, DOI:10.1021/CG4014 448, 2014.

Schmitt, C. G., Heymsfield, A. J., Connolly, P., Järvinen, E., and Schnaiter, M.: A global view of atmospheric ice particle complexity, Geophysical Research Letters, 43, DOI:10.1002/2016GL071 267, 2016.

Schnaiter, M., Järvinen, E., Vochezer, P., Abdelmonem, A., Wagner, R., Jourdan, O., Mioche, G., Shcherbakov, V. N., Schmitt, C. G., Tricoli, U., et al.: Cloud chamber experiments on the origin of ice crystal complexity in cirrus clouds, Atmospheric Chemistry and Physics, 16, 5091–5110, DOI:10.5194/ACP–16–5091–2016, 2016.

Schrom, R. S., van Lier-Walqui, M., Kumjian, M. R., Harrington, J. Y., Jensen, A. A., and Chen, Y.-S.: Radar-Based Bayesian Estimation of Ice Crystal Growth Parameters within a Microphysical Model, Journal of the Atmospheric Sciences, 78, 549–569, 10.1175/jas–d–20–0134.1, https://doi.org/10.1175%2Fjas-d-20-0134.1, 2021.

Skrotzki, J.: High-accuracy multiphase humidity measurements using TDLAS: application to the investigation of ice growth in simulated cirrus clouds, Ph.D. thesis, 2012.

Skrotzki, J., Connolly, P., Schnaiter, M., Saathoff, H., Möhler, O., Wagner, R., Niemand, M., Ebert, V., and Leisner, T.: The accommodation coefficient of water molecules on ice–cirrus cloud studies at the AIDA simulation chamber, Atmospheric Chemistry and Physics, 13, 4451–4466, DOI:10.5194/ACP–13–4451–2013, 2013.

Spichtinger, P. and Krämer, M.: Tropical tropopause ice clouds: a dynamic approach to the mystery of low crystal numbers, Atmospheric Chemistry and Physics, 13, 9801–9818, DOI:10.5194/ACP–13–9801–2013, 2013.

https://doi.org/10.5194/acp-2022-733
Preprint. Discussion started: 23 November 2022

Vautard, R. and Ghil, M.: Singular spectrum analysis in nonlinear dynamics, with applications to paleoclimatic time series, Physica D: Nonlinear Phenomena, 35, 395–424, DOI:10.1016/0167–2789(89)90 077–8, 1989.

Voigtländer, J., Chou, C., Bieligk, H., Clauss, T., Hartmann, S., Herenz, P., Niedermeier, D., Ritter, G., Stratmann, F., and Ulanowski, Z.: Surface roughness during depositional growth and sublimation of ice crystals, Atmospheric Chemistry and Physics, 18, 13 687–13 702, DOI:10.5194/ACP–18–13 687–2018, 2018.

Wagner, R., Benz, S., Bunz, H., Möhler, O., Saathoff, H., Schnaiter, M., Leisner, T., and Ebert, V.: Infrared optical constants of highly diluted sulfuric acid solution droplets at cirrus temperatures, The Journal of Physical Chemistry A, 112, 11 661–11 676, DOI:10.1021/jp8066 102, 2008.

Wagner, R., Linke, C., Naumann, K.-H., Schnaiter, M., Vragel, M., Gangl, M., and Horvath, H.: A review of optical measurements at the aerosol and cloud chamber AIDA, Journal of Quantitative Spectroscopy and Radiative Transfer, 110, 930–949, DOI:10.1016/J.JQSRT.2009.01.026, 2009.

Wood, S. E., Baker, M. B., and Calhoun, D.: New model for the vapor growth of hexagonal ice crystals in the atmosphere, Journal of Geophysical Research: Atmospheres, 106, 4845–4870, DOI:10.1029/2000JD900 338, 2001.

Zhang, C. and Harrington, J. Y.: Including surface kinetic effects in simple models of ice vapor diffusion, Journal of the Atmospheric Sciences, 71, 372–390, DOI:10.1175/JAS–D–13–0103.1, 2014.

Zhang, C. and Harrington, J. Y.: The effects of surface kinetics on crystal growth and homogeneous freezing in parcel simulations of cirrus, Journal of the Atmospheric Sciences, 72, 2929–2946, DOI:10.1175/JAS–D–14–0285.1, 2015.